Fermi National Accelerator Laboratory

FERMILAB-Pub-89/214-A
October 1989

THE GRAND UNIFIED PHOTON SPECTRUM
A Coherent View of the Diffuse Extragalactic Background Radiation

M. TED RESSELL[1,3]

and

MICHAEL S. TURNER[1,2,3]

[1] *Department of Astronomy and Astrophysics*
The University of Chicago
Chicago, IL 60637-1433

[2] *Department of Physics and The Enrico Fermi Institute*
The University of Chicago
Chicago, IL 60637-1433

[3] *NASA/Fermilab Astrophysics Center*
Fermi National Accelerator Laboratory
Batavia, IL 60510-0500

Abstract. We present in a coherent fashion the spectrum of diffuse extragalactic background radiation (DEBRA) at wavelengths from 10^5cm to 10^{-24}cm. Each wavelength region, from the radio to ultra-high energy photons and cosmic rays, is treated both separately and as part of the grand unified photon spectrum (GUPS). A discussion of, and references to, the relevant literature for each wavelength region is included. This review should provide a useful tool for those interested in diffuse backgrounds, the epoch of galaxy formation, astrophysical/cosmological constraints to particle properties, exotic early Universe processes, and many other astrophysical and cosmological enterprises. As a worked example, we derive the cosmological constraints to an unstable-neutrino species (with arbitrary branching ratio to a radiative decay mode) that follow from the GUPS.

To appear in Comments on Astrophysics.

INTRODUCTION

Observation of the diffuse extragalactic background radiation (DEBRA) at various wavelengths provides a unique window on various astrophysical, cosmological, and particle physics phenomena. The existence of the cosmic microwave background radiation (CMBR) with a temperature of 2.74K is well established and, perhaps, provides the strongest evidence for the hot big bang cosmology. Deviations of this radiation from a thermal spectrum and from spatial anisotropy are expected to provide a wealth of information concerning a variety of cosmological problems, including galaxy formation, star formation, and the properties of relic elementary particles. Some theories of structure formation predict the existence of a diffuse radiation at the infrared and optical wavelengths from the first burst of star formation as primeval galaxies formed.[1] In the x-ray and γ-ray regions there is an, as yet, unexplained diffuse background. Any relic particle species that has a radiative decay mode should contribute to the diffuse background, and hence measurements of the diffuse background can be used to discover or to set useful limits to the masses and couplings of such a particle species. Included in the list of relic particles whose existence or properties can be so probed are axions, neutrinos, photinos, and gravitinos. As a worked example we will consider the constraints that apply to a relic neutrino species with an arbitrary branching ratio to a radiative decay mode. Finally, numerous exotic sources for high energy photons—including superconducting cosmic strings—have been and continue to be suggested.

Since there are a number of uses for a compilation of the various diffuse background measurements we have attempted to review and present all the relevant data in the most simple, coherent, and useful manner. Each spectral region is treated separately, the reliability of various measurements are commented upon, and an annotated guide to the literature is provided. Whenever there is, as yet, no definitive data we have attempted to place the best upper limits to the flux provided by other existing data. Finally, we have presented all the data in a consistent set of units: energy flux per unit area per unit time per unit energy per unit solid angle (in cgs units). This corresponds to

$$I_E \equiv \frac{d\mathcal{F}_E}{dAdtdEd\Omega} \ \left(\mathrm{erg\,cm^{-2}s^{-1}erg^{-1}sr^{-1}}\right). \tag{1}$$

It is a simple matter to convert to two other forms of the differential flux often found in the literature I_λ and I_ν:

$$I_\lambda \equiv \frac{d\mathcal{F}_E}{dAdtd\lambda d\Omega} = \frac{hc}{\lambda^2} I_E$$

$$I_\nu \equiv \frac{d\mathcal{F}_E}{dAdtd\nu d\Omega} = hI_E.$$

In addition, the differential particle number flux

$$\frac{d\mathcal{F}_\gamma}{dAdtdEd\Omega} \ \left(\mathrm{cm^{-2}s^{-1}erg^{-1}sr^{-1}}\right) \tag{2}$$

is related to I_E by

$$\frac{d\mathcal{F}_\gamma}{dAdtdEd\Omega} = \frac{I_E}{E} = \frac{\lambda}{E^2} I_\lambda = \frac{1}{hE} I_\nu.$$

Finally, integral fluxes (either number or energy) are sometimes of use:

$$\frac{d\mathcal{F}(>E)}{dAdtd\Omega} \equiv \int_E^\infty \frac{d\mathcal{F}(E')}{dAdtdEd\Omega} dE'.$$

Supposing that

$$\frac{d\mathcal{F}}{dAdtdEd\Omega} = cE^{-n},$$

it follows that

$$\frac{d\mathcal{F}}{dAdtdEd\Omega} = \frac{(n-1)}{E} \frac{d\mathcal{F}(>E)}{dAdtd\Omega},$$

valid for $n > 1$. The following is a brief list of useful conversion factors:

$$1 \text{ Jansky } = 10^{-23} \text{erg cm}^{-2}\text{s}^{-1}\text{Hz}^{-1}$$

$$h^{-1} \left(1 \text{ Watt m}^{-2}\text{Hz}^{-1}\text{sr}^{-1}\right) = 1.509 \times 10^{29} \text{erg cm}^{-2}\text{s}^{-1}\text{erg}^{-1}\text{sr}^{-1}$$

$$\left(\frac{\lambda^2}{hc}\right) \left(1 \text{ erg cm}^{-2}\text{s}^{-1}\text{sr}^{-1}\text{Å}^{-1}\right) = \left(\frac{\lambda}{\text{Å}}\right)^2 5.034 \times 10^7 \text{erg cm}^{-2}\text{s}^{-1}\text{erg}^{-1}\text{sr}^{-1}$$

$$\left(\frac{\lambda^2}{hc}\right) \left(1 \text{ erg cm}^{-2}\text{s}^{-1}\text{sr}^{-1}\text{Å}^{-1}\right) = \left(\frac{\text{erg}}{E}\right)^2 1.986 \times 10^{-8} \text{erg cm}^{-2}\text{s}^{-1}\text{erg}^{-1}\text{sr}^{-1}$$

$$1 \text{ GeV } = 1.602 \times 10^{-3} \text{erg}$$

$$h = 6.626 \times 10^{-27} \text{erg Hz}^{-1}$$

$$hc = 1.986 \times 10^{-16} \text{erg cm } = 1.986 \times 10^{-8} \text{erg Å}$$

$$\hbar c = 1.973 \times 10^{-14} \text{ GeV cm}.$$

$$1 \text{ sr} = 3.283 \times 10^3 \text{ sq deg} = 4.255 \times 10^{10} \text{ sq arcsec}$$

Finally, "diffuse background" means different things in different circumstances. For example, it can refer to a background of unresolved, discrete sources, e.g., the contribution of QSO's to the x-ray background or the extragalactic cosmic rays, or to an intrinsically diffuse background produced by relic-particle decays or radiation scattered and thermalized by dust. In all instances DEBRA refers to extragalactic, rather than galactic, radiation.

RADIO (10^2cm – 10^5cm)

The radio region for which there is data spans the wavelengths from 10^5cm to 10^2cm. At wavelengths longer than about 1 km the opacity of the ISM is very large due to free-free absorption by electrons. Therefore, there are no measurements of the diffuse extragalactic radiation at wavelengths significantly longer than this. Accordingly, $\lambda \sim 1$ km constitutes the long wavelength limit to our spectrum. Unlike most other spectral regions that we will

discuss there have not been measurements in the radio recently. The data we discuss is quite firm as it has stood the test of time. In the region from 6.5×10^4cm to 3.7×10^2cm we have used the data of Clark, Brown, and Alexander,[2] and for wavelengths shorter than this we have chosen the data of Bridle.[3]

The diffuse background in the radio is thought to be comprised of three components: synchrotron radiation from the galactic disk; similar radiation from the halo; and the diffuse extragalactic background radiation due to the integrated emission of all unresolved extragalactic radio sources. It is difficult to separate the three components from one another, and so we have chosen to present the total flux observed in this region as opposed to various authors' estimates of the purely extragalactic component. The data we display is taken from the region near the north galactic pole, and thus it should have the least amount of contamination from the disk component of the diffuse radiation. It should, however, be considered as a combination of galactic and extragalactic radiations, and thus as a very firm limit to the DEBRA. The radio data are summarized in Figure 1.

MICROWAVE and SUBMILLIMETER (10^{-2}cm – 10^2cm)

Unlike the radio, the microwave and submillimeter portion of the DEBRA has been the subject of intense, ongoing research. This is due, of course, to the presence of the relic radiation from the hot big bang which dominates this region of the spectrum. Since the surface of last scattering for the CMBR is the Universe at a red shift of about 1100 and an age of a few-hundred-thousand years, this radiation provides valuable information about the early history of the Universe. The ongoing research is of two types: study of the spatial anisotropy; and study of the spectral shape. Here we are concerned with the spectral measurements. For a review of the anisotropy data we refer the reader to the excellent reviews by Partridge[4] or Wilkinson.[5]

The microwave and submillimeter region of the spectrum extends from wavelengths of 10^2cm to 10^{-2}cm. Measurements of the spectrum of the CMBR are generally reported as an equivalent black body temperature. The energy flux received from a black body that fills the aperture of the antenna is

$$I_E(BB) = \frac{2\nu^3}{c^2}\left[\exp(h\nu/kT) - 1\right]^{-1}; \tag{3}$$

it follows directly that the equivalent thermodynamic temperature of a source with flux I_E is

$$T_{equiv} = \frac{(h\nu/k)}{\ln\left(1 + 2\nu^3/c^2 I_E\right)}. \tag{4}$$

A useful review that details the general methods used in spectral measurements, as well as containing most of the recent measurements, is that of Richards.[6] Before the recent rocket flight of Matsumoto, et al.,[7] Smoot and collaborators[8] found that all measurements of the CMBR in the wavelength range of 0.1 cm to 50 cm were consistent with that of a black body spectrum at temperature $T_{CMBR} = 2.74 \pm 0.02$K. For completeness, we have also

included a somewhat older result at $\lambda \simeq 75\,\mathrm{cm}$; see Weiss[9] for details. At wavelengths longer than 100 cm the galactic background overwhelms the CMBR (see Figure 1). For purposes of comparison we have plotted a black body spectrum of this temperature along with the observational data. Because of the great importance of the CMBR there is a wealth of experimental data for this region of the spectrum; the above mentioned reviews by Richards[6] and Smoot, et al.[8] contain most of the recent data and a rather complete survey of the literature. The experimentalists working in this spectral region are generally very careful in estimating their errors and so the data is generally quite trustworthy. We have summarized the existing data in Figure 2.

A great deal of excitement has recently been generated by the submillimeter measurements of Matsumoto, et al.[7] Their data indicate a deviation from a purely Planckian spectrum on the Wein side of the blackbody spectrum, corresponding to an energy excess amounting to about 10% of that in the CMBR. The deviation is clearly visible in Figure 2. We caution that because of the low flux on the Wein side of the spectrum there is always the possibility that the effect could be instrumental; another rocket flew the same instrument this past September and the data should soon be analyzed. In addition, Cosmic Background Explorer (COBE) is scheduled to fly this November. We also mention that a similar deviation has been seen by Gush,[10] although his experiment had instrumental problems for which he had to correct. A number of theoretical models have been proposed to explain the submillimeter excess including neutrino decays, other relic particle decays, dust emission, and decay of vacuum energy.[11,14] None of the models yet discussed seems completely plausible or compelling. If the distortion is real, the enormous energy budget strongly suggests that the explanation involves fundamental physics—e.g., the decay of some relic species. We should know soon!

In closing, we mention that study of the CMBR is a most active and important area of ongoing cosmological research. Additional measurements of the Rayleigh-Jeans region are being carried out by Levin, et al.[12] and De Amici, et al.;[13] these measurements are important because they provide the opportunity to accurately determine the temperature of the CMBR over two decades in wavelength, and in so doing serve to severely constrain any model of spectral distortion. The COBE satellite will provide high accuracy measurements over a large region of the spectrum. We currently have a good view of the night sky at microwave wavelengths, and it should only continue to improve.

INFRARED ($1\,\mu\mathrm{m} - 100\,\mu\mathrm{m}$)

The infrared (IR) region of the DEBRA is one of great cosmological interest; however, it is one of the most difficult regions to study owing to the enormous opacity of the Earth's atmosphere and ubiquitous dust. Many interesting and important cosmological and astrophysical events taking place between red shift $z \sim$ few to 1000 should contribute to the background of diffuse IR radiation. These sources include pop III stars, galaxy formation, dust-filled galaxies, decaying relic particles, etc. (see e.g. Bond, Carr, and Hogan;[14] McDowell;[15] Rowan-Robinson and Carr;[16] Carr,[17] and references therein). One

might expect it to be a simple matter to compare the predictions to the observations, and thereby test the multitude of cosmological scenarios. However, this is not the case because of the difficulty in interpreting the observations. This difficulty is summed up in a single word, "dust." Technology has advanced to the point where instrumental contamination can be accurately corrected for; however, every observation is contaminated by interplanetary (zodiacal) and interstellar dust emission. Thus, every measurement of the extragalactic component depends upon modeling these contributions and then subtracting them from the total flux to obtain the residual DEBRA flux.

We will take the IR portion of the spectrum to include the wavelengths from 10^{-2}cm (100 μm) to 10^{-4}cm (1 μm). For the majority of the data we present the extragalactic component has been obtained by removing *estimates* of dust emission. Therefore, the reported fluxes are dependent upon the models for dust emission that the investigators use; one may wish to refer to the original papers to see what procedures were used to obtain the results quoted here. In some cases no attempt was made to extract the extragalactic contribution to the flux, and we have used the measurement itself as an upper limit to the diffuse flux.

In the region near 100 μm there are two data sets to consider.[7,18,19] The first is that from the rocket flight of Matsumoto, et al.[7] On the same rocket flight that revealed the deviation from a Planck spectrum in the submillimeter portion of the CMBR, Matsumoto, et al.[7] also obtained measurements in three narrow IR bands centered at wavelengths of 262 μm, 137 μm, and 102 μm. They find that their data are well fit by interstellar dust at a temperature $T_{ISD} \sim 20$ K. They are presently attempting to extract the extragalactic component from these data, and results should be forthcoming.[20] For the moment, their data should be taken to be an upper limit to any diffuse background. The second data set is from IRAS observations.[18,19] At 100 μm Boulanger and Perault[19] have corrected the IRAS data using a particular dust emission model to derive a value for the residual DEBRA. They detail their procedure, and are careful to state that the inherent uncertainties associated with their model are as large as the residual flux itself. Their derived extragalactic flux at $100\,\mu m$ lies substantially below the 102 μm measurement of Matusmoto, et al.[7] At 60 μm Rowan-Robinson and Carr[16] have used another subtraction scheme to obtain the value of I_E that we have used here. Once again we caution that the theoretical uncertainties are at least as large as the deduced DEBRA. Finally, in the region from 50 μm to 10 μm the only measurements that exist are for the total IR flux, and no attempt has been made to extract the diffuse component. To set our upper limits we have used the measurements of Hauser, et al.[18] at the galactic poles and earlier measurements of Soifer, Houck, and Harwitt.[21]

From 1 μm – 10 μm, commonly referred to as the "near IR," it is possible to attempt absolute measurements of the DEBRA, although dust emission is still a problem. Observations of the DEBRA are quite interesting in this region as it is possible that such radiation includes a component from the red shifted light associated with the initial epoch of galaxy formation. The majority of the data we have shown in the near IR is from the

rocket flight of Matsumoto, Akiba, and Murakami[22] (also see Matsumoto[23]). Here too, one must correct for dust emission to obtain a residual isotropic component that may be extragalactic in origin. This experiment had some difficulty with contamination from rocket exhaust; nonetheless, the authors feel confident that the signal detected at 2.2 μm is real. However, the other detections are not as firm. For comparison, we have included two other measurements. The first by Boughn and Kuhn[24] is an upper limit to the DEBRA at 2.2 μm. The second is a measurement at 2.4 μm by Hofmann and Lemke.[25] With this measurement, we have used the *total* measured flux as the upper limit for the error bar in order to give the reader an idea of the amount of dust emission that must be removed from the data (typically a factor of $\sim$ 10 higher than the diffuse flux that is derived). In conclusion, in the IR our knowledge of the diffuse extragalactic spectrum is rapidly improving; however, one must still treat the results with care as they are very dependent upon the dust emission models that are used to extract the extragalactic component.

OPTICAL AND ULTRAVIOLET ($10\text{Å} - 10^4\text{Å}$)

Observers still detect more photons in the optical than in any other part of the spectrum; however, due to the relatively narrow bandwidth of the optical, $\Delta\lambda/\lambda \sim 1$, we will consider it together with the more extensive ultraviolet (UV) band. In keeping with our rather rough definitions of spectral regions we will take the optical/UV to extend from about 10^{-4}cm (10,000Å) to about 10^{-7}cm (10Å). In the usual astronomical parlance this includes the optical, UV, far UV, extreme UV, and a portion of the soft x-ray band.

There have been a variety of searches for the optical component of the DEBRA. As yet, no detection has been claimed, and so we present only upper limits. In comparing the data one must deal with the S_{10} unit, which is defined differently by different authors. (For reference Lang[26] defines the S_{10} unit as one 10th magnitude star per square degree, while Toller[27] defines it as 1 $S_{10}(V)_{G2IV} = 1.2 \times 10^{-9}\text{erg cm}^{-2}\text{s}^{-1}\text{Å}^{-1}\text{sr}^{-1}$ at 4400Å.) For the sake of the reader's (as well as our own) sanity we have converted to our cgs flux units. We have included 4 upper limits to the DEBRA in the optical in Figure 4. They are: Boughn and Kuhn[24] at 6500Å; Dube, Wickes, and Wilkinson[28] at 5115Å; Toller[27] at 4400Å; and Spinrad and Stone[29] at 4000Å. The different authors have chosen to deal with background subtraction with different methods, and we refer the reader to the cited articles for details regarding this point.

From the end of the optical (near 3000Å) to the Lyman limit (912Å) there are a number of claimed detections of the DEBRA. Observations at these wavelengths are especially interesting because neutrinos with cosmologically interesting masses could decay and produce a diffuse background.[30] Unfortunately the observations are not of the sensitivity required to reach the intensity levels predicted by the simplest models, where neutrino decay proceeds through the usual weak interactions. (In more exotic models with horizontal or family symmetries, it may be possible that neutrinos or other particles have sufficiently short lifetimes to be of interest; see below.) Due to the opacity of the atmosphere at these wavelengths, observations must be made with satellite-borne instruments.

This also largely circumvents the problem of airglow. Unfortunately, there are a number of other possible "contaminants" that must be carefully removed from the data before a true estimate of the DEBRA can be made. These contaminants are discussed in detail by Paresce and Jakobson,[31] and they include: zodiacal light, backscatter of radiation off interstellar gas, and hot stars in the field of view. Many observers now feel that they have these problems under control, and that they can make reliable measurements of the UV background radiation. That is not to say that this point is without controversy; see e.g. Martin and Bowyer.[32] (This paper also reports several measurements in this region of the spectrum and provides a good discussion of the effect of galactic evolution upon the UV component of DEBRA.) In any case, the reader should be aware that the reported DEBRA measurements are a only small fraction of the total signal detected.

To summarize the data we have shown; we have used the data from the review of Paresce and Jakobson[31] at 3300Å and 2980Å. The data at 2200Å and 1690Å are from observations made by Joubert, et al.[33] using the D2B Aura satellite. The points at 1440Å and 1715Å are from a rocket flight by Anderson, et al.[34] as revised by Feldman, Brune, and Henry.[35] (This data is also presented in Henry.[36]) Observations at 1360Å were carried out by Weller,[37] using an instrument on the Solrad 11 satellite. We also include a measurement that provides an upper limit in the region from 1200Å to 500Å. Using the UV spectrometer aboard the Voyager 2 spacecraft Holberg found no residual signal after removing the interplanetary lines.[38] Finally, we include data for two regions that have been surveyed spectroscopically. First, in the region 1200Å $< \lambda <$ 1700Å, Murthy, et al.[39] carried out a survey with 17Å resolution using a shuttle-borne spectrometer (this group also has data extending up to 3100Å but it is not yet published). (Hurwitz, Martin, and Bowyer[40] flew a similar instrument on the same shuttle flight and are said to have found similar flux levels.) In the region 1700Å $< \lambda <$ 2850Å we have included the 50Å resolution data of Tennyson, et al.[41] In both cases we have displayed the data with a box that indicates the uncertainities. For more details, the reader should consult the original papers.

Shortward of 912Å is known as the extreme UV (EUV). Because of the large cross section for absorption by interstellar HI (neutral hydrogen) there is little chance of ever acquiring a spectrum of the DEBRA. (The ISM is known to be patchy, and it is possible that one could probe the DEBRA in the EUV by looking through a "hole".) The absorption cross section decreases as E^{-3}, $\sigma(E) \simeq 6 \times 10^{-23}(E/\mathrm{keV})^{-3}\,\mathrm{cm}^2$, and so the interstellar medium becomes transparent again at wavelengths of order 100Å. Measurements between 912Å and 100Å can be used to learn a great deal about the gas content of our own galaxy. The upper limit of Holberg[38] extends from 1200Å down to 500Å. The other points we show are from Stern and Bowyer[42] and Paresce and Stern,[43] and they extend from about 700Å down to about 20Å ($E \simeq 18$ eV to 0.62 keV). The shortest wavelength measurements are actually in the soft x-ray band. The data shortward of 912Å are reliable, but because of strong absorption by the local ISM, they must be considered as a local flux. At the highest energies ($\lambda \lesssim 100$Å), the data should provide a reliable upper limit to the DEBRA. The

measurements of the optical and UV are displayed in Figure 4.

X RAY and γ RAY (1 keV − 100 MeV)

The diffuse extragalactic x-ray and γ-ray backgrounds are very well measured in the energy range of 1 keV to 100 MeV ($\lambda \simeq 10^{-7}\,\mathrm{cm}$ to $\lambda \simeq 10^{-12}\,\mathrm{cm}$). Since these backgrounds are similar in nature we have displayed them together in Figure 5. Following the conventional nomenclature, we will refer to keV photons as x rays and MeV (and above) photons as γ rays. The x-ray background has been reviewed extensively; see, e.g., the excellent reviews by Boldt.[44] As he discusses, discrete sources such as quasars and Seyfert galaxies contribute a substantial fraction of the cosmic x- and γ-ray backgrounds. It is also believed by many, based upon the shape of the x-ray spectrum, that another substantial part may be due to a hot ($T \sim 10^9$ K) diffuse plasma. There is no consensus as to the relative proportions of the two contributions—or if there is another significant, yet unidentified, component.

The x-ray spectrum from 1 keV to 3 keV is fit by a simple power law[45]

$$I_E = 7.7 \left(\frac{E}{1\,\mathrm{keV}}\right)^{-0.4} \mathrm{erg\,cm^{-2}s^{-1}erg^{-1}sr^{-1}}. \tag{5}$$

From 3 keV to 50 keV Marshall, et al.[46] have found their data to be well fit by an optically-thin, thermal bremsstrahlung model with temperature $kT = 40 \pm 5\,\mathrm{keV}$. Gruber, et al.[47] confirm this form of the spectrum in the energy interval from 15 keV to 100 keV, except they derive $kT = 43 \pm 1\,\mathrm{keV}$. In Figure 5 we have displayed the representation used by Boldt,[44]

$$I_E = \mathrm{A} \left(\frac{E}{3\,\mathrm{keV}}\right)^{-\alpha} \exp(-E/kT) \tag{6}$$

where $\mathrm{A} = 5.6\ \mathrm{erg\,cm^{-2}s^{-1}erg^{-1}sr^{-1}}$, $kT = 40$ keV, and $\alpha = 0.29$. To give an impression of the size of the measurement uncertainties we have also shown the data of Gruber, et al.[47] (without error bars since they are quite small) in this range. From 100 keV to 1 MeV we have shown the data of Gruber, et al.[47] (with error bars).

In the γ-ray portion of the spectrum from 0.3 MeV to 10 MeV we have used the data of Trombka, et al.[48] The central line shown is the data, and the upper and lower lines represent the 1σ error limits. We call the reader's attention to the relatively good agreement between this data set and that of Gruber et al.[47] where they overlap. There are no definite detections between 10 MeV and 35 MeV; however, we have included 2 upper limits, which indicate that there are no big surprises (see Trombka et al.[48]). Finally, we display the SAS II data of Fichtel, Simpson, and Thompson[49] which extends from 35 MeV to 100 MeV. For a discussion of this portion of the spectrum we refer the reader to Fichtel[50] and the earlier review of Silk.[51] We have displayed the data of Fichtel, et al.[49] as a parallelogram that specifies the 1σ allowed region in the $I_E - E$ plane (also see Rothschild et al.[52]). Finally, there is also one measurement from the COS-B satellite at 70 MeV, but we defer comment upon this until the next section.

HE, VHE, UHE, and UHE γ RAYS and COSMIC RAYS (E > 100 MeV)

The region of the spectrum from 100 MeV to the very highest energies observed, about 10^{20}eV, is a very interesting one. Unfortunately, a diffuse flux is extremely difficult to measure. In fact, at these energies there are no claimed measurements of a diffuse *extragalactic*—as opposed to a galactic—component. There are a number of detections of a diffuse component that can be used as upper limits to any extragalactic component. Even so, there are large parts of the electromagnetic spectrum that have never been surveyed in any manner whatsoever. For example, Dogiel, et al.[53] point out that there has never been an experiment to search for cosmic γ rays in the energy range 4–400 GeV, despite the fact that this region is a potentially interesting one (e.g., dark-matter decays and annihilations in the halo[53a]). (The EGRET instrument on the Gamma Ray Observatory (GRO) will explore the region of 20 MeV to 30 GeV when GRO is launched next year. More ambitious experiments that probe the region of 1 GeV to 1 TeV have been proposed for the Freedom Space Station.) Because of the paucity of data, we have turned to cosmic ray (CR) measurements to provide *absolute* upper limits. (Except for the muon content and shower shape, at these energies there is very little difference between photon- and hadron-induced showers. For reference, where both γ and CR data are available, the γ-ray flux is at least 3 to 4 orders of magnitude smaller.) We have scrounged for *any* γ-ray data available, and the reader should be forewarned that much of the data is open to interpretation. Let us discuss the data that we have chosen to display in Figure 6.

The γ-ray data in the range from 70 MeV to 3.3 GeV are very reliable. We have used the COS-B data for the galactic anti-center region (Sacher and Schönfelder;[54] also see Mayer-Hasselwander, et al.[55]). This data is confined to a wedge $\pm$ 30 degrees from the galactic plane that is far removed from the galactic center. It should be relatively free of "galactic contamination," and at the least provide a reasonably good upper limit to any extragalactic flux. (For reference, the ratio of the flux in the direction of the galactic center to that in the direction of the galactic anti-center is about 5).

From 3 GeV to 1 TeV there is very little data available. Moreover, we were unable to locate any suitable data for energies of 3 to 30 GeV. From 30 GeV to 1 TeV we mention the measurements of Nishimura, et al.[56] The group flew a balloon-borne instrument at an atmospheric depth of about 4 g cm^{-2} for the purpose of measuring the CR electron flux. In so doing they detected a flux of atmospheric γ rays with spectrum given by

$$I_E \simeq 1.2 \times 10^{-6} \left(\frac{100\,\mathrm{GeV}}{E} \right)^{1.75} \mathrm{erg\,cm^{-2}s^{-1}erg^{-1}sr^{-1}}. \qquad (7)$$

They were able to attribute the entire flux to secondary γ rays from π^0 decays. The π^0's are produced by the interactions of primary hadronic CR's in the atmosphere. At the very least, this data provides an absolute upper limit to any diffuse flux of γ rays because of the shallow atmospheric depth of the experiment. (The interaction length for γ rays in the atmosphere is about 47 g cm^{-2},[57,58] much less than the 4 g cm^{-2} depth of the instrument.)

Since cosmic γ rays of energies greater than 100 GeV behave much like hadronic CR's in their interactions with matter, they should have been detected in any experiment that measures the total CR flux. Thus, we have used the total CR flux above 100 GeV (from Linsley[59] and Hillas[60]) as a very firm upper limit to the γ-ray flux above 100 GeV. Moreover, since the CR spectrum is of interest in its own right we have presented this data in a rather complete manner. We have relied upon the summary given by Hillas.[60] (Other extensive reviews exist; see e.g., Watson[61] and Linsley.[59]) The Hillas compilation includes data from the Proton 4 satellite and the Tien Shan, Akeno, Haverah Park, and Yakutsk extensive air shower arrays. The reader is referred to his review for a more complete bibliography.

The very highest energy cosmic ray data, $10^{17}\,\mathrm{eV} \lesssim E \lesssim 10^{20}\,\mathrm{eV}$, comes from the Fly's Eye array[62] as well as the Haverah Park and Yakutsk arrays mentioned above. There is some evidence in the Fly's Eye data for the so-called Griesen cut off at an energy of about 7×10^{19}eV; the cut off arises as this is the threshold energy for π meson production off CMBR photons, $p + \gamma_{3K} \longrightarrow p + \pi$. The other feature in the CR data is the "knee" at an energy of about 10^{15}eV, which (probably) traces to the large gyro radius for cosmic rays above this energy which allows them to more easily escape magnetic confinement within the Galaxy.

It is the very tough job of the γ-ray astronomer to separate out the small residual flux of primary γ rays from the large "background" of hadronic cosmic rays. This is difficult to do for two reasons. First, the γ-ray flux expected is only 10^{-3} to 10^{-4} of the CR flux, which is itself falling rapidly with energy.[63,64,65] Second, in order to do so one must differentiate between γ- and hadron-induced showers, and the differences are subtle—shower development and shape, and muon content. Photon-induced showers are expected to be narrower and muon-poor. Moreover, because photons maintain their directionality (whereas charged CR's are strongly influenced by the galactic magnetic field), much of the γ-ray astronomy effort is devoted to searching for point sources. The "telescope," whether an atmospheric Čerenkov mirror or a particle detector array, is pointed toward the source for a time and then taken "off source" for an equal time, and the two measurements are subtracted to obtain the source signal. (See Weekes[66] for a lucid and in depth description of the experimental techniques.) While this technique is useful for eliminating background, it also eliminates the DEBRA component. There are, however, several measurements of a diffuse component associated with the galactic disk and in some directions on the sky that we will present.

Weekes[66] has reviewed much of the data we present at energies above 1 TeV; we will only mention the measurements that are pertinent to the diffuse background. First, a few general points. All of the data are presented as integral fluxes, i.e., $I_E(> E)$. All the data from extensive air shower (EAS) arrays are selected based upon being muon-poor showers. Monte Carlo calculations indicate that EAS's initiated by primary γ rays should be deficient in muons by a factor of about 30 as compared to hadron-initiated showers. (Whether or not γ-induced showers are truly muon poor is presently a matter of debate.

In the past few years, a number of point-source detections have been made[67,68] where the shower is *apparently* not muon-poor. Since the sources involved, Cyg X-3 and Her X-1, are at distances of many kpc's it is certain that the primary particle must be neutral—to maintain its directionality—and long lived suggesting that it is indeed a photon. If the observations are correct, either the primary particle is not a photon, or photon-induced showers at energies greater than about 1 TeV are not really muon poor.)

Next, the mean-free path for primary γ's with energies of 10^{14} to 10^{15} eV is very short, $\lambda_{mfp} \sim 10's$ of kpcs, because this energy is the threshold for e^+e^- pair production off CMBR photons ($\gamma + \gamma_{3K} \longrightarrow e^+ + e^-$). For higher-energy photons the mean-free path grows slowly but does not really reach cosmological distances even at energies of 10^{20}eV. Thus, there is little hope of measuring a truly *extragalactic* background at these energies. (For a discussion of this issue see Protheroe,[69] and Zdziarski and Svensson.[70]) Finally, because fluxes and event rates are small, the statistical significance of any of the measurements discussed is far from being secure—but the data we mention here are the best presently available.

Now the individual observations of the diffuse γ-ray background. For energies greater than 0.5 TeV and 1.8 TeV we have shown two differential measurements (on minus off) in the galactic plane made by Fazio, et al.[71] For energies above 30 TeV we use the all-sky flux of μ-poor showers recorded at the Chacaltaya EAS array in the 1960's as an upper limit to any diffuse γ-ray flux.[72] For energies above 100 TeV we also show the diffuse flux of muon- and hadron-poor showers found over a large region of the sky by Suga, et al.[73] in a re-analysis of the Chacaltaya data. Gawin, et al.[74] determined an upper limit to the photon flux at energies above 800 TeV from the μ-poor EAS data available at the time. Weekes[66] argues that the most reliable data comes from the Tien Shan EAS which is for energies of 1 PeV (10^{15}eV) and above.[75] The Tien Shan array has excellent particle discrimination and they have selected only those shower events with very few muons *and* hadrons to derive an all-sky diffuse γ-ray flux. Their flux corresponds to 5 γ rays in 12,900 hours of observation. At energies above 2×10^{16}eV Dzikowski, et al.[76] have measured a diffuse flux in the galactic plane, and we use their measurement as an upper limit to the diffuse extragalactic γ-ray flux. The highest energy point, $E \geq 10^{17}$eV, is from the Yakutsk EAS array and is based upon *one* μ-poor shower.[77] All of the claimed detections of a diffuse γ-ray flux correspond to about 0.1% of the CR flux—in agreement with the theoretical expectations mentioned above. Not only are there no definitive measurements of the diffuse γ-ray flux at energies above 10 GeV, but also the very interesting question of whether γ-induced showers are muon poor has yet to be answered.

For purposes of comparison we have included rough representations of the CR electron (plus positron) flux, the atmospheric-muon flux, and the atmospheric-neutrino flux in Figure 6. The electrons (and positrons) are generally believed to be cosmic ray primaries, while the muons and neutrinos are produced by the interaction of hadronic CR primaries in the Earth's atmosphere (through π, K, etc. meson decays). The spectrum of electrons and positrons extends from 1 MeV to 2 TeV and is a compilation of data taken by Meyer,[78]

Golden, et al.,[79] Tang,[80] and Nishimura, et al.[56] The spectrum is dominated by electrons but positrons do a contribute at the 10% level; see e.g., Müller and Tang.[81] (Most of the positron flux is believed to arise from the decays of mesons that are produced by CR interactions with the ISM; more exotic sources have also been suggested: e.g., dark matter annihilations in the halo.) We present the sea level atmospheric muon data from Allkofer[82] in the energy region from 0.2 GeV to 10^5 GeV. It consists of the differential measurements from 0.2 GeV to 1 TeV of Allkofer, et al.[83] and an integral spectrum converted to a differential spectrum (using a spectral index of n = 3.57) from 1 TeV to 100 TeV.

Finally, the atmospheric-neutrino spectrum includes $\nu_e, \overline{\nu}_e, \nu_\mu$, and $\overline{\nu}_\mu$ neutrinos and is the *theoretical* spectrum based upon known nuclear and particle physics and the measured flux of muons at sea level. From 10 MeV to 10 GeV we have used the calculations of Gaisser and Stanev,[84] and from 10 GeV to 10^7 GeV those of Volkova.[85] The two calculations are in reasonable agreement in their region of overlap, but note the slight jump in I_E. The atmospheric-neutrino flux is an important background for large underground detectors such as IMB, Kamiokande, Soudan, Frejus, NUSEX, and KGF. Moreover, the flux of atmospheric neutrinos has been measured in several of these experiments; see Svoboda, et al.,[87] Krishnaswamy, et al.,[88] and Reines, et al.[89] Finally, Krauss, et al.[86] have calculated the background of antineutrinos expected from radioactive decays within the Earth and various astrophysical sources (Sun, supernovae, etc.).

To summarize our review of the DEBRA, we present in Figure 7 "the grand unified photon spectrum" (or GUPS). From the GUPS one can clearly see that most of the diffuse photons in the Universe reside in the CMBR. In terms of the energy content of the diffuse background it is a close—and still undecided—contest between the CMBR and the submillimeter/IR region of the spectrum. While the photon flux at energies above 1 eV is falling rapidly, this part of the spectrum may contain important information and clues concerning interesting cosmological as well as contemporary astrophysical events.

A WORKED EXAMPLE: CONSTRAINTS TO UNSTABLE NEUTRINOS

To illustrate one of the uses of the GUPS we will consider the wide variety of constraints to the mass and lifetime of an unstable neutrino species that derive from it. If neutrinos are massive, then the different flavor eigenstates (e, μ, and τ) can—and indeed are likely to—mix, and transitions between different neutrino types are possible. Thus, a massive neutrino is expected to be unstable. Within the context of the standard electroweak interactions, a massive neutrino can decay, $\nu_H \longrightarrow \nu_L + \gamma$, with a lifetime

$$\tau_\nu \sim 10^{27} \sin^{-2}(2\theta)(m_\nu c^2/\,\mathrm{eV}\,)^{-5}\mathrm{sec} \tag{8}$$

(ν_H = "heavier" neutrino, ν_L = "lighter" neutrino); neutrinos heavier than 1 MeV can decay, $\nu_H \longrightarrow \nu_L + e^+ + e^-$, with a lifetime

$$\tau_\nu \sim 10^{24} \sin^{-2}(2\theta)(m_\nu c^2/\,\mathrm{eV}\,)^{-5}\mathrm{sec}. \tag{9}$$

Further, if there exist new flavor changing (or horizontal) interactions characterized by an energy scale, F, a heavy neutrino can decay $\nu_H \longrightarrow \nu_L + X$ (where X is some unspecified scalar particle, e.g., majoron, familon, etc.), with a lifetime

$$\tau_\nu \sim \mathrm{F}^2 m_\nu^{-3} \simeq 10^{22} (\mathrm{F}/10^{10}\ \mathrm{GeV})^2 (m_\nu c^2/\mathrm{eV})^{-3} \mathrm{sec}. \tag{10}$$

In most models with horizontal (or family) interactions, the energy scale F must be greater than about 10^9 GeV to be consistent with the absence of various flavor-changing neutral current processes.

So we see that massive neutrinos are very likely to be unstable—and with long lifetimes. Thus their decays are probably beyond the "reach" of terrestrial laboratories. Because a long-lived neutrino with mass in the 30 eV range is cosmologically interesting many groups have searched for neutrino-decay produced photons in the UV portion of the spectrum; see e.g., De Rújula and Glashow,[30] Holberg and Barber,[90] and Henry.[37] (For reference, $\Omega_{\nu\overline{\nu}} = m_\nu/91h^2$ eV where $\Omega_{\nu\overline{\nu}}$ is the fraction of critical density contributed by relic neutrinos and here h is the Hubble constant in units of 100 km sec^{-1} Mpc^{-1}.) There has yet to be any convincing evidence for relic neutrino decay, and so the present data serve to provide upper limits to the lifetime, τ_ν, of the neutrino. Since the anticipated lifetimes are long and usually inaccessible in the laboratory, astrophysics and cosmology can provide unique information as to the possibility of neutrino decay—even if neutrino masses are not cosmologically interesting. In this section we will consider an unstable neutrino species of mass m_ν and lifetime τ_ν that has a branching ratio, B_r, to a radiative decay mode. The "source of the neutrinos" for our cosmological laboratory is the big bang, and we will assume the "standard" relic abundance for a neutrino species (see below). In addition we shall assume that these relic neutrinos are uniformly distributed—if they should be clustered with galaxies or galaxy clusters the constraints that follow are even more stringent. We will use the GUPS to exclude regions of the mass-lifetime plane (which depend upon B_r).

The limits that we obtain depend upon the epoch during which the neutrinos decay. To simplify the analysis, we consider four qualitatively different lifetime regimes: 1) lifetimes longer than the age of the universe, t_U; 2) lifetimes shorter than t_U but longer than the age of the Universe at matter-radiation decoupling (red shift $z \simeq 1100$); 3) lifetimes between the time of matter-radiation decoupling and the time at which double-Compton scattering ($\gamma + e^- \longrightarrow e^- + \gamma + \gamma$) becomes effective at thermalizing the decay photons ($z \simeq 10^7$); 4) lifetimes such that the neutrino species is relativistic at decay.

For an unstable neutrino species that has a lifetime longer than $t_U \sim 4 \times 10^{17}$sec relic neutrinos are still decaying today and produce an intensity

$$I_E = \frac{n_\nu c}{4\pi\tau_\nu H_0} \left(\frac{E_\gamma}{m_\nu c^2/2}\right)^{3/2} B_r, \tag{11}$$

where we have assumed a flat Universe and a two-body decay so that each decay-produced photon has an energy $E_\gamma = m_\nu c^2/2$. (The decay photons are mono-energetic when produced; however, because they decay over a range of red shifts, there is a spectrum of

photons at the present epoch.) The present neutrino number density, n_ν, depends upon whether the neutrinos were relativistic or non-relativistic at the time when they decoupled. A light neutrino species ($m_\nu \ll 1$ MeV) decouples at a temperature of a few MeV, when it is still relativistic, and such a species today is about as abundant as photons: $n_\nu = 115\,\mathrm{cm}^{-3}$. A heavy neutrino species ($m_\nu \gg 1$ MeV) decouples when it is non-relativistic ($kT_d \simeq m_\nu c^2/20$), and its present relic abundance is approximately

$$n_\nu = 1.78 \times 10^{-5} \left(\frac{m_\nu c^2}{1\,\mathrm{GeV}}\right)^{-3} \left[1 + \frac{3\ln(m_\nu c^2/\,\mathrm{GeV})}{15}\right] \mathrm{cm}^{-3}. \tag{12}$$

(For the derivation and discussion of these results see Kolb and Turner.[91])

For simplicity we will assume that the dividing line between a "heavy" and a "light" neutrino species is $m_\nu c^2 = 1\,\mathrm{MeV}$. It is now straightforward to constrain the quantity τ_ν/B_r by comparing the predicted flux with that observed and requiring that the predicted flux of decay photons not exceed the observed flux. (Note, except for a narrow wavelength interval around the Lyman limit, the Universe is transparent to the decay-produced photons.) We display the results of this exercise in Figure 8 for neutrino masses in the range $10^{-3}\,\mathrm{eV} < m_\nu c^2 < 100\,\mathrm{GeV}$. The upper mass limit is determined by the fact that n_ν as a function of m_ν must change form for neutrinos more massive than the Z^0 boson; moreover, it is not obvious that a neutrino more massive than a few hundred GeV can be self-consistently incorporated into the electroweak theory. The lower limit follows from the fact that these neutrinos are relativistic today and must be treated separately, which we shall do shortly. Finally, we mention that long-lived neutrinos of mass between $91h^2\,\mathrm{eV}$ and 2 GeV are forbidden by another very familiar cosmological argument; namely the fact that their present mass density would be excessive.

For a neutrino species that has a lifetime shorter than t_U but longer than the age of the Universe at matter-radiation decoupling, $t_{DEC} \simeq 5.6 \times 10^{12}(\Omega_0 h^2)^{-1/2}$ sec, a slightly different analysis must be performed. The main differences are: (i) because all the relic neutrinos have decayed by the present, only B_r and m_ν are relevant; (ii) the expression for I_E is simpler because each relic neutrino produces one photon, from which it follows that

$$\mathcal{F}_\gamma = \int I_E \frac{dE}{E} = \frac{n_\nu c}{4\pi} B_r. \tag{13}$$

Here n_ν is the number density that the neutrinos would have today had they not decayed and $\mathcal{F}_\gamma$ is the number flux of relic photons ($\mathrm{cm}^{-2}\mathrm{sr}^{-1}\,\mathrm{sec}^{-1}$). Again, assuming a two-body decay, the decay-produced photons are mono-energetic, with energy $E_\gamma \simeq m_\nu c^2/(1+z_d)$, where the red shift at the epoch of decay is

$$(1+z_d) = 4.8 \times 10^9 (\tau_\nu/\,\mathrm{sec})^{-1/2} \quad (t_d \lesssim t_{EQ}) \tag{14a}$$

$$(1+z_d) = 3.8 \times 10^{11} (\tau_\nu/\,\mathrm{sec})^{-2/3} (\Omega_0 h^2)^{-1/3} \quad (t_d \gtrsim t_{EQ}) \tag{14b}$$

where t_{EQ} is the age of the Universe at the epoch of matter-radiation equality: $t_{EQ} = 4.4 \times 10^{10}(\Omega_0 h^2)^{-2}$ sec. Since the decays occur over a red shift interval $\Delta z/z \sim \mathcal{O}(1)$, $\Delta E_\gamma/E_\gamma \sim$

$\mathcal{O}(1)$, and $I_E \simeq \mathcal{F}_\gamma = B_r n_\nu c/4\pi$. Using this approximation we can obtain a limit to B_r for neutrino masses in the range $10^{-3}\,\mathrm{eV} < m_\nu c^2 < 100\,\mathrm{GeV}$ by comparing the predicted flux to the GUPS (as we did before). Our constraint is shown in Figure 9.

For an unstable neutrino species that decays when it relativistic, a slightly different chain of reasoning applies. Such a neutrino species will have maintained the thermal equilibrium distribution it had when it decoupled, but with a red shifted temperature: $T_\nu(t) = T_d R_d/R(t)$. Thus it will have an energy density given by

$$\rho_\nu = \frac{7}{8} a T_\nu^4 = \frac{7}{8}\left(\frac{4}{11}\right)^{4/3} a T_\gamma^4 \simeq 0.23 a T_\gamma^4, \tag{15}$$

where the factor of $7/8$ comes from Fermi-Dirac statistics and the factor of $(4/11)^{4/3}$ arises because the photon temperature increases relative to the neutrino temperature at the epoch of e^+e^- annihilation, which occurs *after* neutrinos decouple from the plasma. Since the energy density in the CMBR is aT_γ^4, it follows that the energy density in neutrino-decay produced photons amounts to $0.11B_r$ times that in the CMBR (assuming that on average each decay-produced photon carries away half the energy of its parent neutrino). These neutrino-decay-produced photons have typical energies that are comparable to, but less than that of, a typical CMBR photon, and the total energy content of the decay-produced photons is about $0.11B_r$. Unless they can be thermalized, or unless $B_r \lesssim 0.1$, unacceptable distortions of the CMBR will result. The decay-produced-photons can be thermalized—as opposed to scattered—only if the decays occur early enough so that the double-Compton process is effective ($t \lesssim t_{DC} \sim 10^6\,\mathrm{sec}$). Thus we can conclude that an unstable neutrino species with $B_r \gtrsim 0.1$ that decays *after* $t = t_{DC} \sim 10^6\,\mathrm{sec}$ and before the present epoch is forbidden on cosmological grounds; the excluded region of the mass-lifetime plane is given by

$$200\,\mathrm{sec}\,/\,\mathrm{eV} \lesssim \tau_\nu/m_\nu c^2 \lesssim 4\times 10^{20}(\Omega_0 h^2)^{1/3}\,\mathrm{sec}\,/\,\mathrm{eV}\,, \tag{16}$$

subject to the condition that the neutrino species be relativistic when it decays, which corresponds to

$$m_\nu c^2 < 3.5\times 10^8 (\Omega_0 h^2)^{-1/3}\left(\frac{\tau_\nu}{\mathrm{sec}}\right)^{-2/3}\ \mathrm{eV} \qquad (\tau_\nu > t_{EQ}), \tag{17}$$

$$m_\nu c^2 < 4.6\times 10^6 \left(\frac{\tau_\nu}{\mathrm{sec}}\right)^{-1/2}\ \mathrm{eV} \qquad (\tau_\nu < t_{EQ}). \tag{18}$$

In Figure 10 we show this constraint (for $\Omega_0 h^2 = 1/4$).

Now consider a neutrino species that decays when it is non-relativistic and has a lifetime in the range $t_{DC} < \tau_\nu < t_{DEC}$. Neutrinos that decay during this epoch will deposit energy into the CMBR that can be scattered but cannot be thermalized because of the ineffectiveness of the double-Compton process. This will result in a CMBR spectrum that is characterized by a Bose-Einstein distribution with non-zero chemical potential. Because the CMBR spectrum is that of a black body to high precision, we can set limits

to combinations of τ_ν, m_ν, and B_r. If we crudely characterize the allowed distortion by requiring that the ratio of energy density in the decay-produced photons to that in the CMBR be less than 0.1, we arrive at the following limits for $m_\nu c^2 < 1$ MeV and $m_\nu c^2 > 1$ MeV respectively:

$$m_\nu c^2 \lesssim 2 \times 10^6 \left(\tau_\nu B_r^2\right)^{-1/2} \text{ eV}\,, \tag{19}$$

$$m_\nu c^2 \gtrsim 8 \times 10^6 \left[1 + \frac{3 \ln(m_\nu c^2 / \text{ GeV})}{15}\right]^{1/2} \left(\tau_\nu B_r^2\right)^{1/4} \text{ eV}\,. \tag{20}$$

The logarithm term in the second expression arises from the formula for the relic abundances of a heavy neutrino species. (We have assumed that the Universe is radiation dominated during the decay epoch; if not previously discussed constraints apply.) This constraint is shown in Figure 10.

The electromagnetic energy released by an unstable neutrino species that decays at a time earlier than about 10^6 sec should become well thermalized so that it will not distort the CMBR. (It will of course increase the entropy of the Universe, however the limit that follows is not particularly severe; see Ref. 91.) For further discussion of the constraints that apply to an unstable neutrino species and a complete list of references, see Ref. 91.

CONCLUDING REMARKS

The diffuse spectrum of electromagnetic radiation extends from 10^5 cm to 10^{-24} cm, some 29 orders of magnitude. It is dominated by the CMBR. With the exception of a small portion of the UV, it provides a unique and very large window on the Universe out to cosmological distances, allowing one to study physical processes as diverse as star formation and relic-particle decays. Two regions of the extragalactic background remain almost unexplored: the IR and that above energies of a few GeV, and both are of great cosmological interest.

In closing, we should mention the earlier reviews of the diffuse background that exist; they include those of Longair,[92] Lequeux,[93] and Shafer.[94] We also caution the reader that our synthesis of the diffuse background data and review of the literature has by no means been exhaustive. Our bibliography, while extensive, is not complete, and we have in most cases deferred to review articles for more complete surveys of the literature.

Acknowledgments

We wish to thank Bill Collins, Rocky Kolb, and Brian Yanny for their valuable assistance. This work was supported in part by the DoE (at Chicago and Fermilab), by NASA (at Fermilab), and by MTR's NASA GSRP fellowship at Chicago.

REFERENCES

1. R.B. Partridge and P.J.E. Peebles, *Astrophys. J.* **147**, 868 (1967).
2. T.A. Clark, L.W. Brown, and J.K. Alexander, *Nature* **228**, 847 (1970).
3. A.H. Bridle, *M.N.R.A.S.* **136**, 14 (1967).
4. R.B. Partridge in *Observational Cosmology: IAU Symposium 124* (Beijing), ed. A. Hewitt, G.R. Burbidge, and L. Fang (D. Reidel, Dordrecht, 1987), pp. 31-53; R.B. Partridge *Rep. Prog. Phys.* **51**, 647 (1988).
5. D.T. Wilkinson in *13th Texas Symposium on Relativistic Astrophysics*, ed. M.P. Ulmer (World Scientific, Singapore, 1987), pp. 209-218.
6. P.L. Richards in *Comets to Cosmology: Proceedings of the Third IRAS Conference* (London), ed. A. Lawrence (Springer-Verlag, Berlin, 1988), pp. 289-296.
7. T. Matsumoto, S. Hayakawa, H. Matsuo, H. Murakami, S. Sato, A.E. Lange, and P.L. Richards, *Astrophys. J.* **329**, 567 (1988).
8. G.F. Smoot, M. Bensadoun, G. Bersanelli, G. De Amici, A. Kogut, S. Levin, and C. Witebsky, *Astrophys. J. (Letters)* **317**, L45 (1987).
9. R. Weiss, *Ann. Rev. Astron. Astrophys.* **18**, 489 (1980).
10. H.P. Gush, *Phys. Rev. Lett.* **47**, 745 (1981).
11. F.C. Adams, K. Freese, J. Levin, and J.C. McDowell, *Astrophys. J.*, in press (1989); J. Bernstein and S. Dodelson, *Phys. Rev. Lett.* **62**, 1804 (1989); J.R. Bond, B.J. Carr, and C.J. Hogan, submitted to *Astrophys. J.* (1989); G.B. Field and T.P. Walker, *Phys. Rev. Lett.* **63**, 117 (1989); K. Freese, F.C. Adams, J.A. Frieman, and E. Mottola, *Nuc. Phys.* **B287**, 797 (1987); M. Fukugita, *Phys. Rev. Lett.* **62**, 1805 (1989); M. Fukugita, et al., *Astrophys. J.* **342**, L1 (1989); C.G. Lacy and G.B. Field, *Astrophys. J.* **330**, L1 (1988).
12. S.M. Levin, C. Witebsky, M. Bensadoun, G. De Amici, A. Kogut, and G.F. Smoot, *Astrophys. J.* **334**, 14 (1988).
13. G. De Amici, G.F. Smoot, J. Aymon, M. Bersanelli, A. Kogut, S.M. Levin, and C. Witebsky, *Astrophys. J.* **329**, 556 (1988).
14. J.R. Bond, B.J. Carr, and C.J. Hogan, *Astrophys. J.* **306**, 428 (1986).
15. J.C. McDowell, *M.N.R.A.S.* **223**, 763 (1986).
16. M. Rowan-Robinson and B.J. Carr, Queen Mary College Preprint (1988).
17. B.J. Carr, in *Comets to Cosmology: Proceedings of the Third IRAS Conference* (London), ed. A. Lawrence (Springer-Verlag, Berlin, 1988), pp. 265-278.
18. M.G. Hauser, et al., *Astrophys. J.* **278**, L15 (1984).
19. F. Boulanger and M. Pérault, *Astrophys. J.* **330**, 964 (1988).
20. A.E. Lange, et al. (to be published).
21. B.T. Soifer, J.R. Houck, and M. Harwitt, *Astrophys. J.* **168**, L73 (1971).
22. T. Matsumoto, M. Akiba, and H. Murakami, *Astrophys. J.* **332**, 575 (1988).
23. T. Matsumoto, in *Comets to Cosmology: Proceedings of the Third IRAS Conference* (London), ed. A. Lawrence (Springer-Verlag, Berlin, 1988), pp. 279-288.

24. S.P. Boughn and J.R. Kuhn, *Astrophys. J.* **309**, 33 (1986).
25. W. Hofmann and D. Lemke, *Astr. Astrophys.* **68**, 389 (1978).
26. K.R. Lang, *Astrophysical Formulae*, (Springer-Verlag, Berlin, 1980), pp. 571-574.
27. G.N. Toller, *Astrophys. J.* **266**, L79 (1983).
28. R.R. Dube, W.C. Wickes, and D.T. Wilkinson, *Astrophys. J.* **232**, 333 (1979).
29. H. Spinrad and R.P.S. Stone, *Astrophys. J.* **226**, 609 (1978).
30. A. De Rújula and S.L. Glashow, *Phys. Rev. Lett.* **45**, 942 (1980).
31. F. Paresce and P. Jakobsen, *Nature* **288**, 119 (1980).
32. C. Martin and S. Bowyer, *Astrophys. J.* **338**, 667 (1989).
33. M. Joubert, J.L. Masnou, J. Lequeux, J.M. Deharveng, and P. Cruvellier, *Astr. Astrophys.* **128**, 114 (1983).
34. R.C. Anderson, W.H. Brune, R.C. Henry, P.D. Feldman, and W.G. Fastie, *Astrophys. J.* **233**, L39 (1979).
35. P.D. Feldman, W.H. Brune, and R.C. Henry, *Astrophys. J.* **249**, L51 (1981).
36. R.C. Henry in *Cosmology and Particles (16th Recontre de Moriond)* ed. J. Audouze, et al. (Singapore National Printers Ltd., Singapore, 1981), pp. 211-229.
37. C.S. Weller, *Astrophys, J.* **268**, 899 (1983).
38. J.B. Holberg, *Astrophys. J.* **311**, 969 (1986).
39. J. Murthy, R.C. Henry, P.D. Feldman, and P.D. Tennyson, *Astrophys. J.* **336**, 954 (1989).
40. M. Hurwitz, C. Martin, and S. Bowyer in preparation.
41. P.D. Tennyson, R.C. Henry, P.D. Feldman, and G.F. Hartig, *Astrophys. J.* **330**, 435 (1988).
42. R. Stern and S. Bowyer, *Astrophys. J.* **230**, 755 (1979).
43. F. Paresce and R. Stern, *Astrophys. J.* **247**, 89 (1981).
44. E. Boldt, *Phys. Rep.* **146**, 215 (1987); E. Boldt, in *Observational Cosmology: IAU Symposium 124* (Beijing), ed. A. Hewitt, G.R. Burbidge, and L. Fang (D. Reidel, Dordrecht, 1987), pp. 611-615.
45. D.A. Schwartz, in *X-Ray Astronomy*, ed. W.A. Baity and L.E. Peterson (Pergamon Press, Oxford, 1979), pp. 453-465.
46. F.E. Marshall, E.A. Boldt, S.S. Holt, R.B. Miller, R.F. Mushotzky, L.A. Rose, R.E. Rothschild, and P.J. Serlemitsos, *Astrophys. J.* **235**, 4 (1980).
47. D.E. Gruber, J.L. Matteson, G.V. Jung, and R.L. Kinzer, *Proc. 19th Internat. Cosmic-Ray Conf.* (La Jolla) **1**, 349 (1985).
48. J.I. Trombka, C.S. Dyer, L.G. Evans, M.J. Bielefeld, S.M. Seltzer, and A.E. Metzger, *Astrophys. J.* **212**, 925 (1977).
49. C.E. Fichtel, G.A. Simpson, and D.J. Thompson, *Astrophys. J.* **222**, 833 (1978).
50. C.E. Fichtel, *Adv. Space Res.* **3**, 5 (1983).
51. J. Silk, *Annual Rev. Astron. Astrophys.* **11**, 269 (1973).
52. R.E. Rothschild, R.F. Mushotzky, W.A. Baity, D.E. Gruber, J.L. Matteson, and L.E. Peterson, *Astrophys. J.* **269**, 423 (1983).

53. V.A. Dogiel, A.P. Kostin, L.V. Kurnosova, L.A. Razorenov, M.A. Rusakovich, N.P. Topchiev, and M.I. Fradkin, *Proc. 20th Internat. Cosmic-Ray Conf.* (Moscow) **2**, 356 (1987).
53a. J. Primack, B. Sadoulet, and D. Seckel, *Ann. Rev. Nucl. Part. Sci.* **38**, 751 (1988).
54. W. Sacher and V. Schönfelder, *Space Science Reviews* **36**, 249 (1983).
55. H.A. Mayer-Hasselwander, et al., *Astr. Astrophys.* **105**, 164 (1982).
56. J. Nishimura, et al., *Astrophys. J.* **238**, 394 (1980).
57. M.S. Longair, *High Energy Astrophysics* (Oxford University Press, Oxford, 1981), pp. 16-58.
58. R. Hiller, *Gamma Ray Astronomy* (Cambridge University Press, Cambridge, 1984), pp. 27-30.
59. J. Linsley, *Proc. 18th Internat. Cosmic-Ray Conf.* (Bangalore) **12**, 135 (1983).
60. A.M. Hillas in *High Energy Astrophysics (19th Recontre de Moriond)* ed. J. Audouze and J. Tran Thanh Van (Frontiéres, Gif sur Yvette, France, 1984), pp. 11-26.
61. A.A. Watson, *Proc. 19th Internat. Cosmic-Ray Conf.* (La Jolla) **9**, 111 (1985).
62. R.M. Baltrusaitis, R. Cady, G.L. Cassiday, R. Cooper, J.W. Elbert, P.R. Gerhardy, S. Ko, E.C. Loh, Y. Mizumoto, M. Salamon, P. Sokolsky, and D. Steck, *Phys. Rev. D* **54**, 1875 (1985).
63. J. Wdowcyzk, and A.W. Wolfendale, *Nature* **305**, 609 (1983).
64. C.L. Bhat, T. Kifune, and A.W. Wolfendale, *Astr. Astrophys.* **159**, 299 (1986).
65. Y. Matsubara, T. Hara, N. Hayashida, M. Honda, T. Kifune, M. Mori, M. Nagano, M.V.S. Rao, and M. Teshima, *J. Phys. G* **14**, 385 (1988).
66. T.C. Weekes, *Phys. Rep.* **160**, 1 (1988).
67. M. Samorski and W. Stamm, *Proc. 18th Internat. Cosmic-Ray Conf.* (Bangalore) **11**, 244 (1983).
68. D.E. Nagle, T.K. Gaisser, and R.J. Protheroe, *Ann. Rev. Nucl. Part. Sci.* **38**, 609 (1988).
69. R.J. Protheroc, *M.N.R.A.S.* **221**, 769 (1986).
70. A.A. Zdziarski and R. Svensson, *Astrophys. J.* **344**, 551 (1989).
71. G.G. Fazio, H.F. Helmken, G.H. Rieke, and T.C. Weekes, *Proc. 11th Internat. Cosmic-Ray Conf.* (Budapest) **1**, 115 (1969).
72. K. Kamata, et al. *Can. J. Phys.* **46**, S72 (1968).
73. K. Suga, et al., *Astrophys. J.* **326**, 1036 (1988).
74. J. Gawin, R. Maze, J. Wdowczyk, and A. Zawadzki, *Can. J. Phys.* **46**, S75 (1968).
75. J.N. Stamenov, S.Z. Ushev, S.I. Nikolsky, and V.I. Yakovlev, *Proc. 18th Internat. Cosmic-Ray Conf.* (Bangalore) **6**, 54 (1983).
76. T. Dzikowski, J. Gawin, B. Grochalska, J. Korejwo, and J. Wdowczyk, *Proc. 19th Internat. Cosmic-Ray Conf.* (La Jolla) **1**, 238 (1985).
77. A.V. Glushkov, N.N. Efimov, N.N. Efremov, I.T. Makarov, M.I. Pravdin, and L.I. Dedenko, *Proc. 19th Internat. Cosmic-Ray Conf.* (La Jolla) **2**, 186 (1985).
78. P. Meyer in *Origin of Cosmic Rays*, ed. J.L. Osborne and A.W. Wolfendale (D. Reidel,

Dordrecht, 1975), pp. 233-266.
79. R.L. Golden, et al., *Astrophys. J.* **287**, 622 (1984).
80. K.K. Tang, *Astrophys. J.* **278**, 881 (1984).
81. D. Müller and K.K. Tang, *Astrophys. J.* **312**, 183 (1987).
82. O.C. Allkofer in *Proceedings of the 1978 DUMAND Summer Workshop*, ed. A. Roberts, (DUMAND, LaJolla, 1979), pp. 13-27.
83. O.C. Allkofer, K. Carstensen, and W.D. Dau, *Phys. Lett.* **36B**, 425 (1971).
84. T.K. Gaisser and T. Stanev, in *Sixth Workshop on Grand Unification*, ed. S. Rudaz and T.F. Walsh (World Scientific, Singapore, 1986), pp. 236-259.
85. L.V. Volkova, *Sov. J. Nucl. Phys.* **31**, 784 (1980).
86. L.M. Krauss, D.N. Schramm, and S.L. Glashow, *Nature* **310**, 191 (1984).
87. R. Svoboda, et al., *Astrophys. J.* **315**, 420 (1987).
88. M.R. Krishnaswamy, et al. *Proc. Roy. Soc. London* **323**, 489 (1971).
89. F. Reines, et al., *Phys. Rev. D* **4**, 80 (1971).
90. J.B. Holberg and H.B. Barber, *Astrophys. J.* **292**, 16, (1985).
91. E.W. Kolb and M.S. Turner *The Early Universe*, (Addison Wesley, Redwood City, 1989), pp. 111-151.
92. M.S. Longair, *Rep. Prog. Phys.*, **34**, 1125 (1971).
93. J. Lequeux in *Physical Cosmology*, ed. R. Balian, J. Audouze, and D.N. Schramm, (North-Holland, Amsterdam, 1980), pp. 5-51.
94. R. Shafer, Ph.D. Dissertation, University of Maryland, NASA TM-85029 (1983).

FIGURE CAPTIONS

Figure 1 — The radio region of the spectrum. Note the long wavelength tail of the CMBR in the lower right corner.

Figure 2 — The microwave/submillimeter region of the spectrum which is dominated by the CMBR. The energy flux from a black body with a temperature 2.74 K is shown for comparison; note the submillimeter excess found by Matsumoto, et al.[7]

Figure 3 — The infrared region of the spectrum. The majority of the measurements have been corrected for galactic dust emission; see text for details.

Figure 4 — The optical and ultraviolet region of the spectrum. Here too the majority of the measurements have had various contaminants removed by modelling.

Figure 5 — The x-ray and γ-ray region of the spectrum (up to an energy of 100 MeV). The curve at upper right is the fit of Boldt[44] joined to the power law fit of Schwartz[45]. The three lines in the center represent the measurements Trombka, et al.[48] with 1 σ error bars. The parallelogram in the lower right hand corner indicates the data of Fichtel, et al.[49] (with 1 σ error flags).

Figure 6 — The γ-ray region of the spectrum ($E \geq 100$ MeV) and the cosmic ray spectrum above 100 GeV. Circles denote the all-particle CR spectrum as summarized by Hillas[60]; triangles the all-particle CR spectrum from the Fly's Eye[62]; and squares the claimed γ-ray fluxes and upper limits using air Čerenkov and muon-poor air shower techniques (see text for details). The solid line is the upper limit to the photon flux from Nishimura, et al.[56] For reference we show the CR $e^{\pm}$ flux, the atmospheric-muon flux, and the atmospheric neutrino flux.

Figure 7 — The grand unified photon spectrum, or GUPS. This figure is a synthesis of Figures 1–6.

Figure 8 — Lifetime/branching ratio constraints for an unstable neutrino species whose lifetime is longer than the age of the Universe. The boundary of the "excluded" region and "allowed" regions is defined by the locus of points (and line segments) that are shown.

Figure 9 — Branching ratio constraint for an unstable neutrino species with lifetime $t_{DEC} < \tau_\nu < t_U$. The boundary of the "excluded" region and "allowed" regions is defined by the locus of points (and line segments) that are shown.

Figure 10 — The constraints that apply to an unstable neutrino species that decays while it is relativistic (dashed line) and one that decays while it is non-relativistic and between decoupling and the epoch that the double-Compton process became ineffective (solid lines). Note, for the former limit the branching ratio B_τ must be $\gtrsim 0.1$, otherwise there is no constraint.

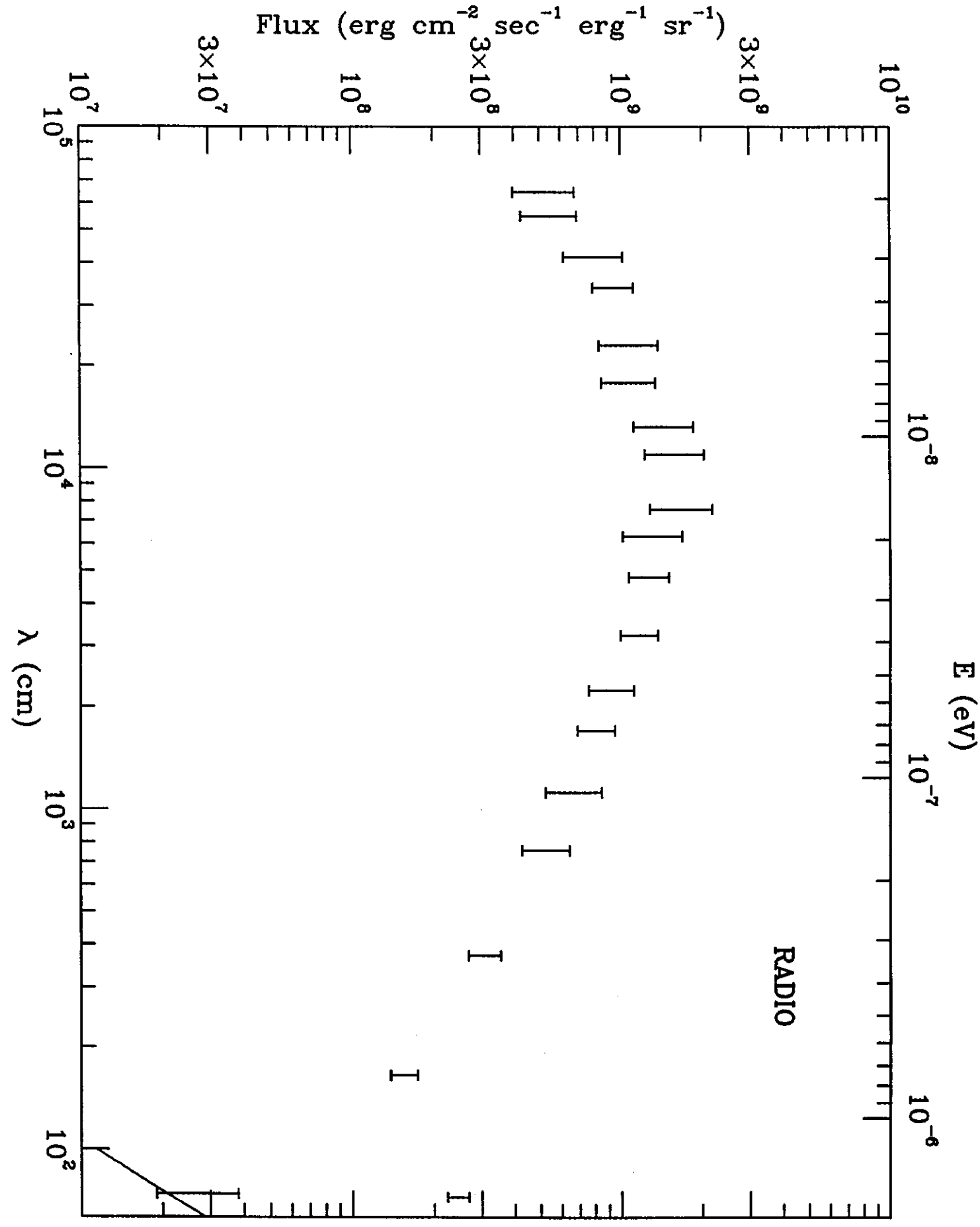
Flux (erg cm^{-2} sec^{-1} erg^{-1} sr^{-1})
10^{7}
3×10^{7}
10^{8}
3×10^{8}
10^{9}
3×10^{9}
10^{10}
10^{5}
10^{4}
10^{3}
10^{2}
λ (cm)
10^{-8}
10^{-7}
10^{-6}
E (eV)
RADIO

FIGURE 1

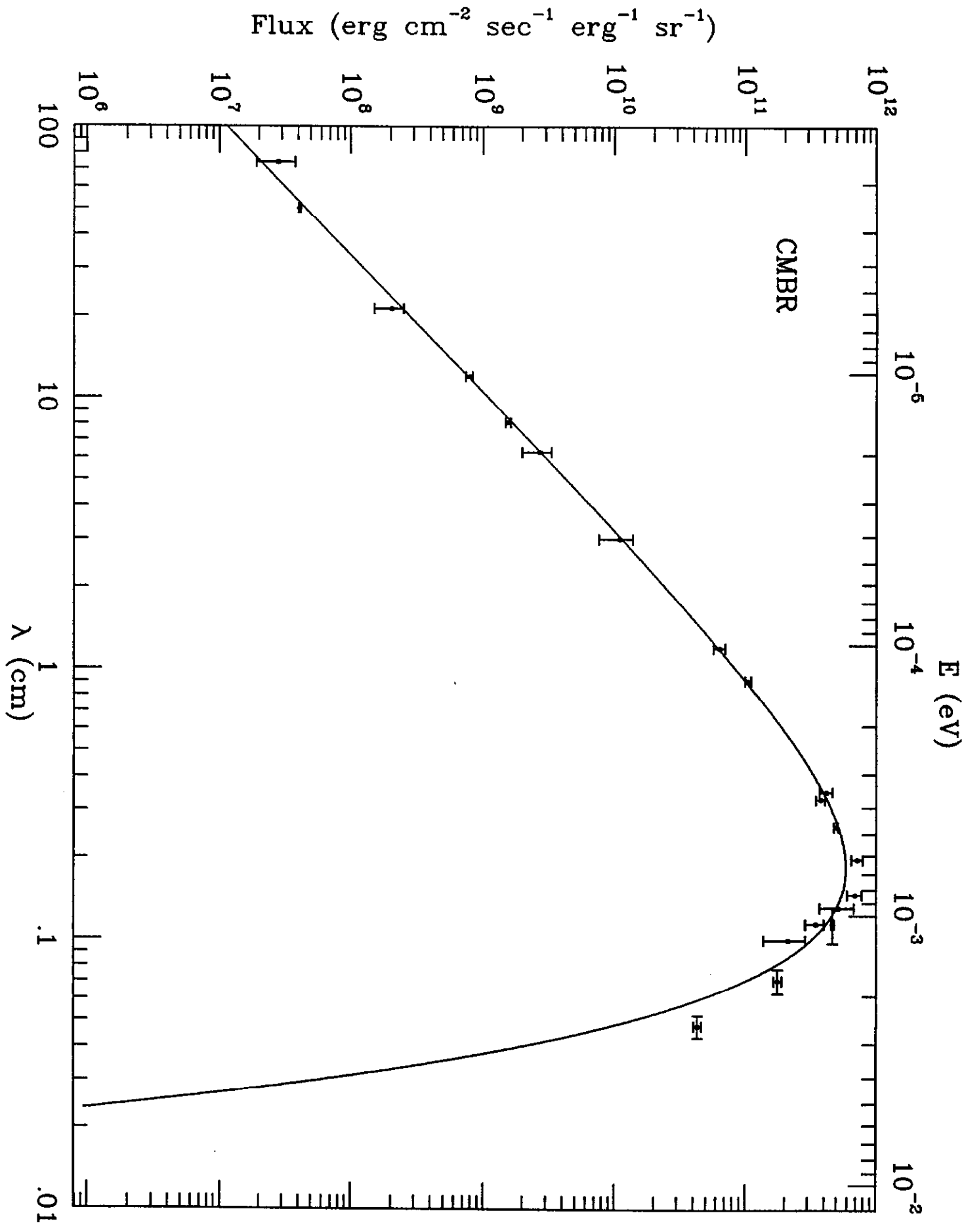
Flux (erg cm^{-2} sec^{-1} erg^{-1} sr^{-1})
10^{6}
10^{7}
10^{8}
10^{9}
10^{10}
10^{11}
10^{12}
100
10
1
.1
.01
λ (cm)
10^{-5}
10^{-4}
10^{-3}
10^{-2}
E (eV)
CMBR

FIGURE 2

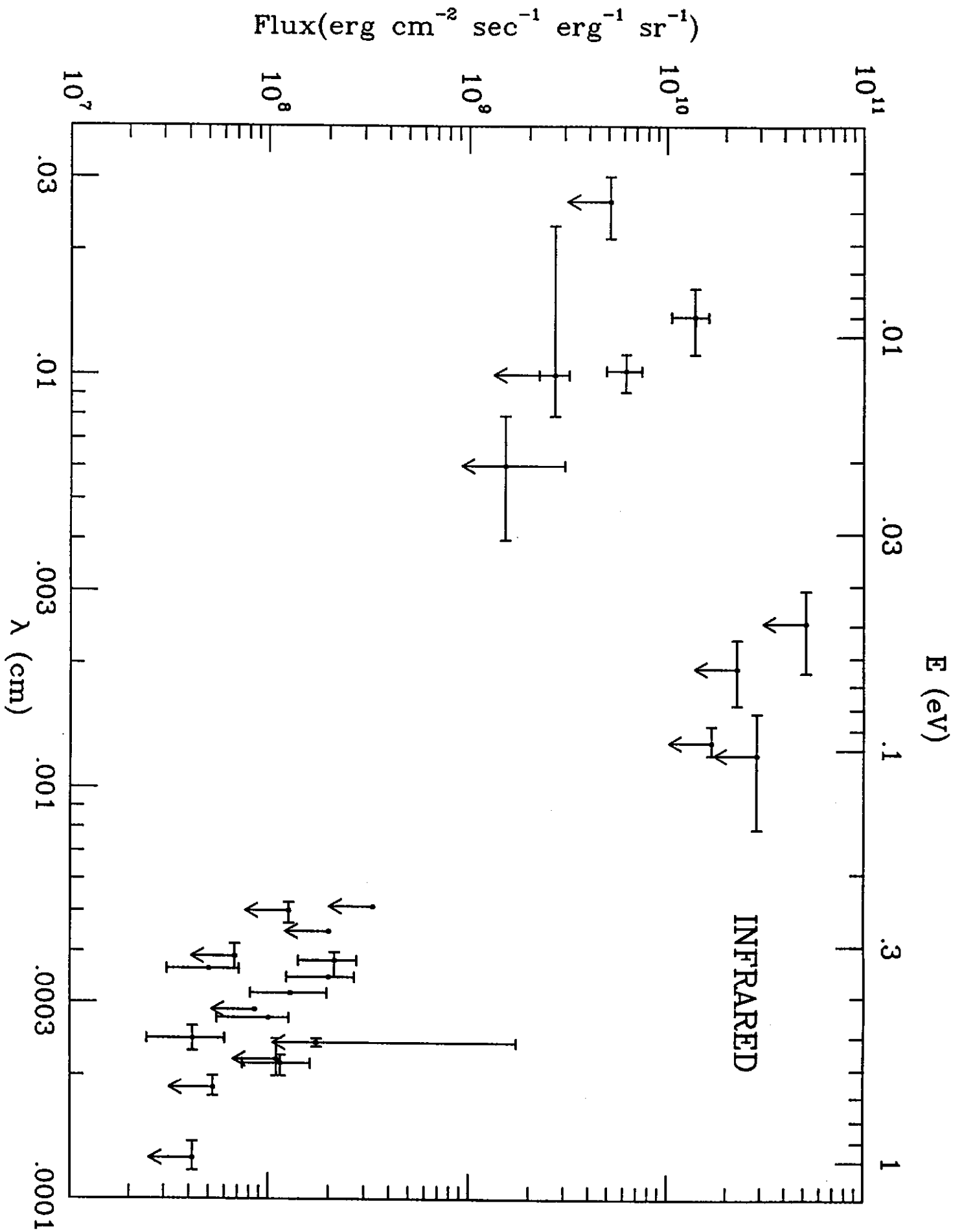
Flux(erg cm^{-2} sec^{-1} erg^{-1} sr^{-1})
10^{7}
10^{8}
10^{9}
10^{10}
10^{11}
.03
.01
.003
.001
.0003
.0001
λ (cm)
.01
.03
.1
.3
1
E (eV)
INFRARED

FIGURE 3

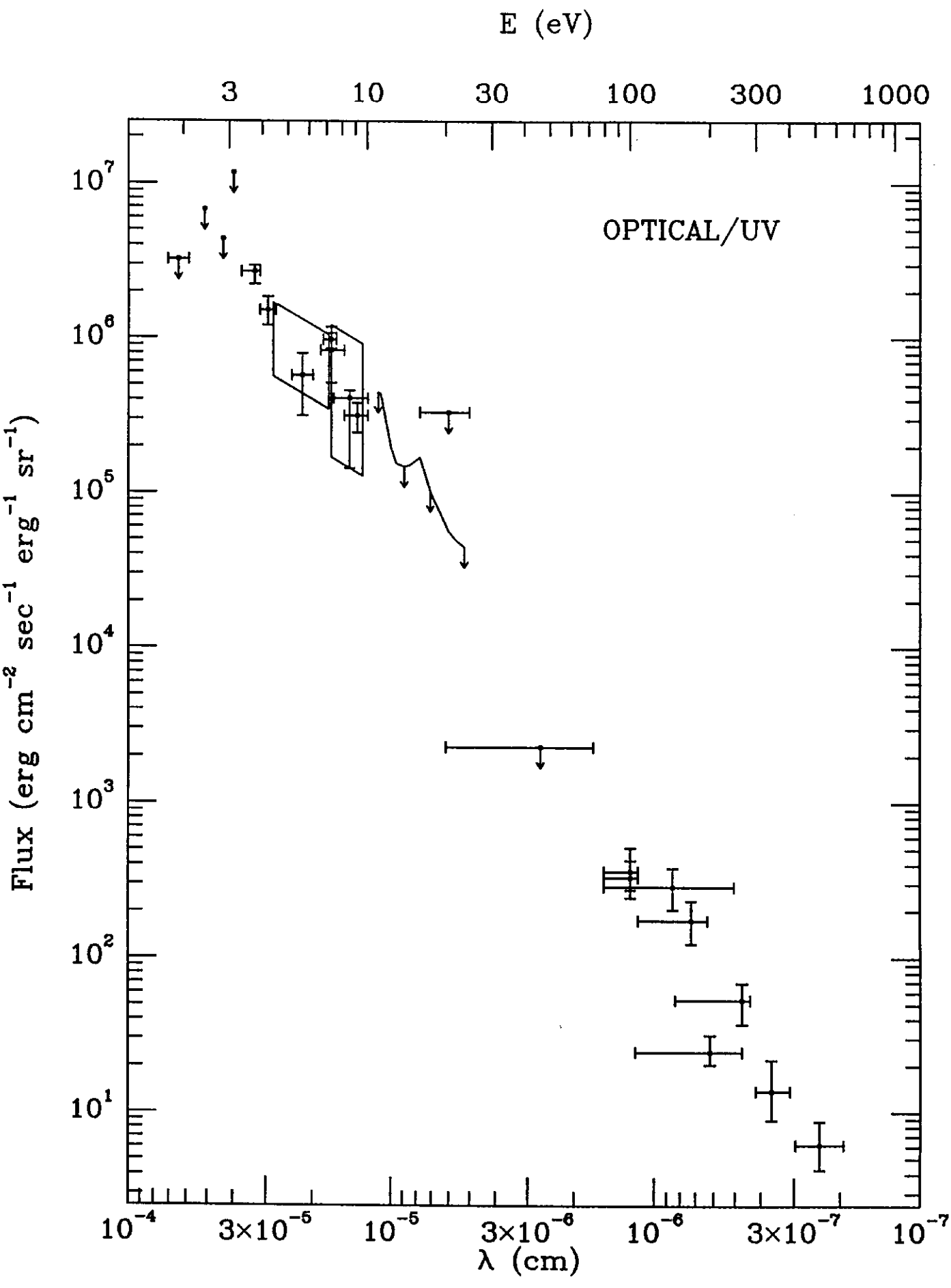
E (eV)
3
10
30
100
300
1000
OPTICAL/UV
Flux (erg cm^{-2} sec^{-1} erg^{-1} sr^{-1})
10^7
10^6
10^5
10^4
10^3
10^2
10^1
10^{-4}
3×10^{-5}
10^{-5}
3×10^{-6}
10^{-6}
3×10^{-7}
10^{-7}
λ (cm)

FIGURE 4

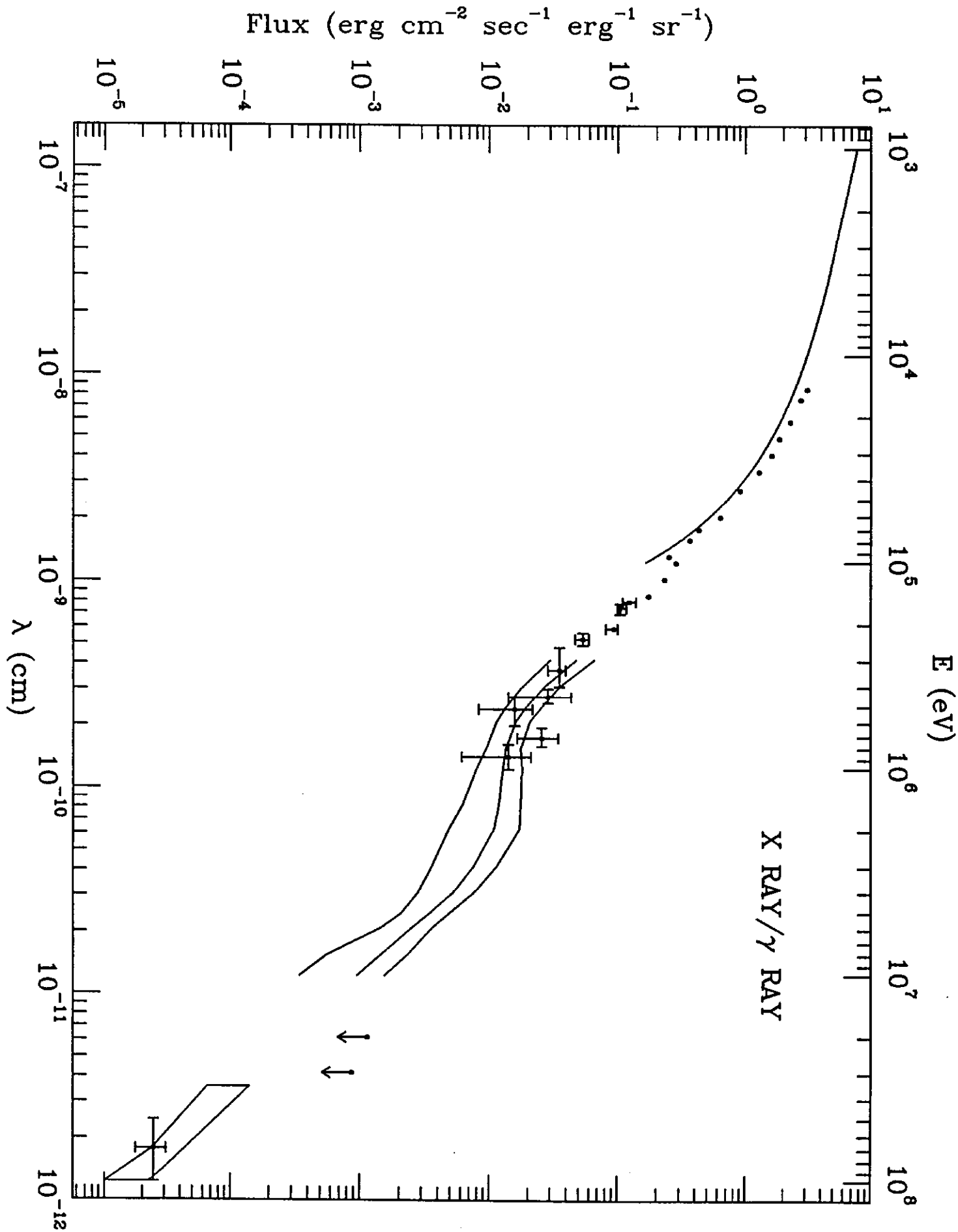
Flux (erg cm^{-2} sec^{-1} erg^{-1} sr^{-1})
10^{-5}
10^{-4}
10^{-3}
10^{-2}
10^{-1}
10^{0}
10^{1}
10^{-7}
10^{-8}
10^{-9}
10^{-10}
10^{-11}
10^{-12}
λ (cm)
10^{3}
10^{4}
10^{5}
10^{6}
10^{7}
10^{8}
E (eV)
X RAY/γ RAY

FIGURE 5

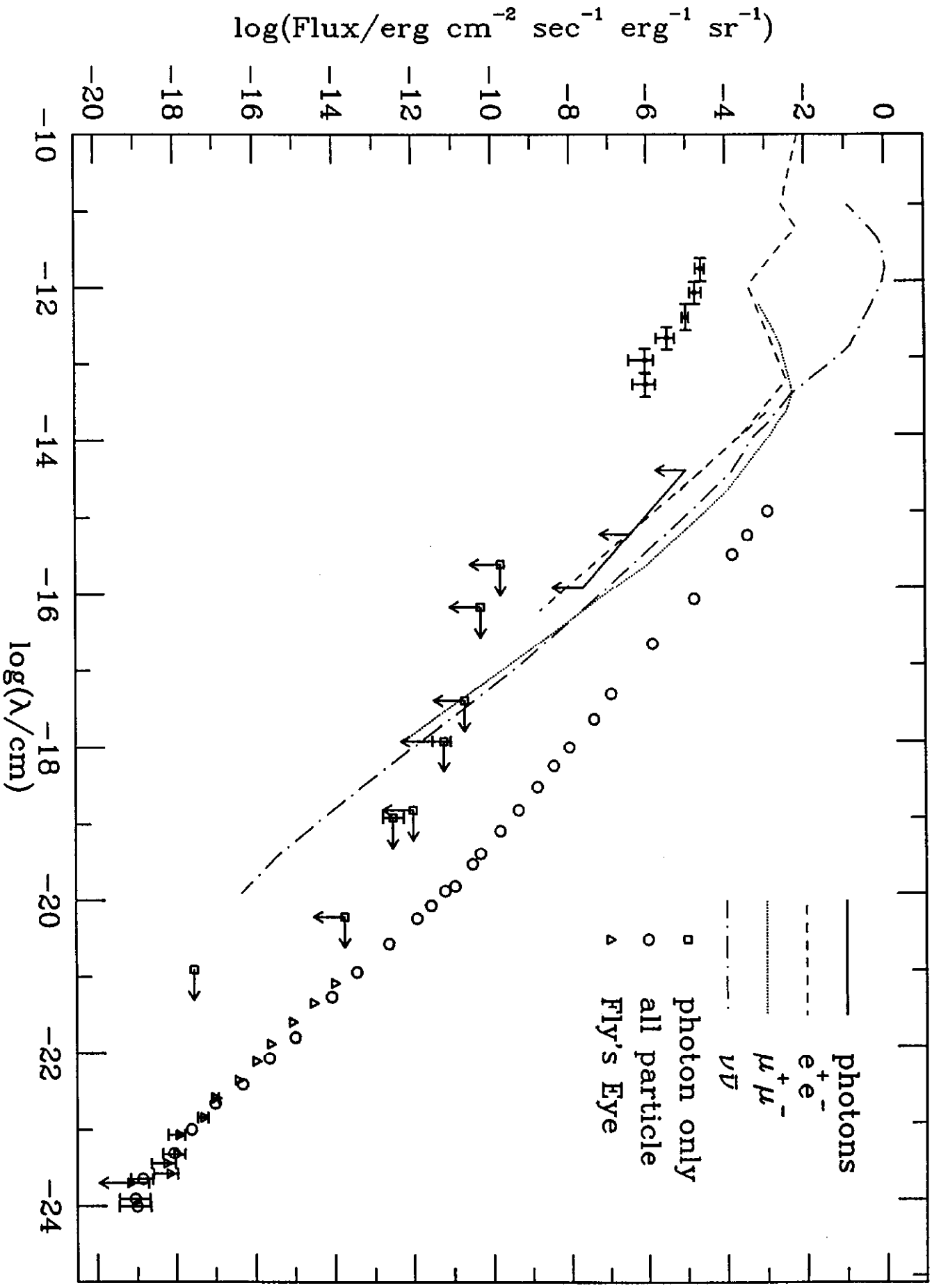
log(Flux/erg cm^{-2} sec^{-1} erg^{-1} sr^{-1})
log(E/eV)
log(λ/cm)
photons
e^+e^-
$\mu^+\mu^-$
$\nu\bar{\nu}$
photon only
all particle
Fly's Eye

FIGURE 6

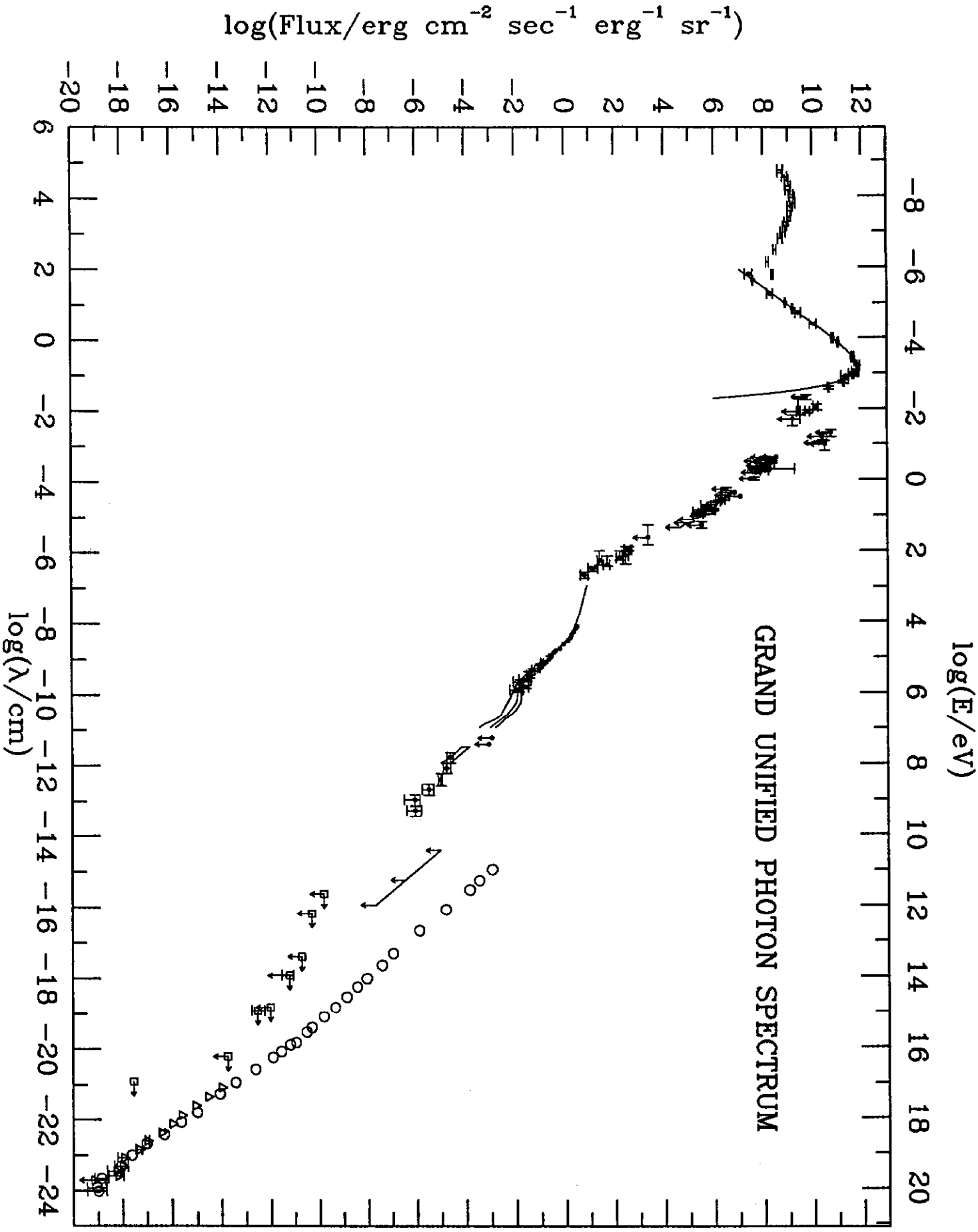
log(Flux/erg cm^{-2} sec^{-1} erg^{-1} sr^{-1})
log(E/eV)
log(λ/cm)
GRAND UNIFIED PHOTON SPECTRUM

FIGURE 7

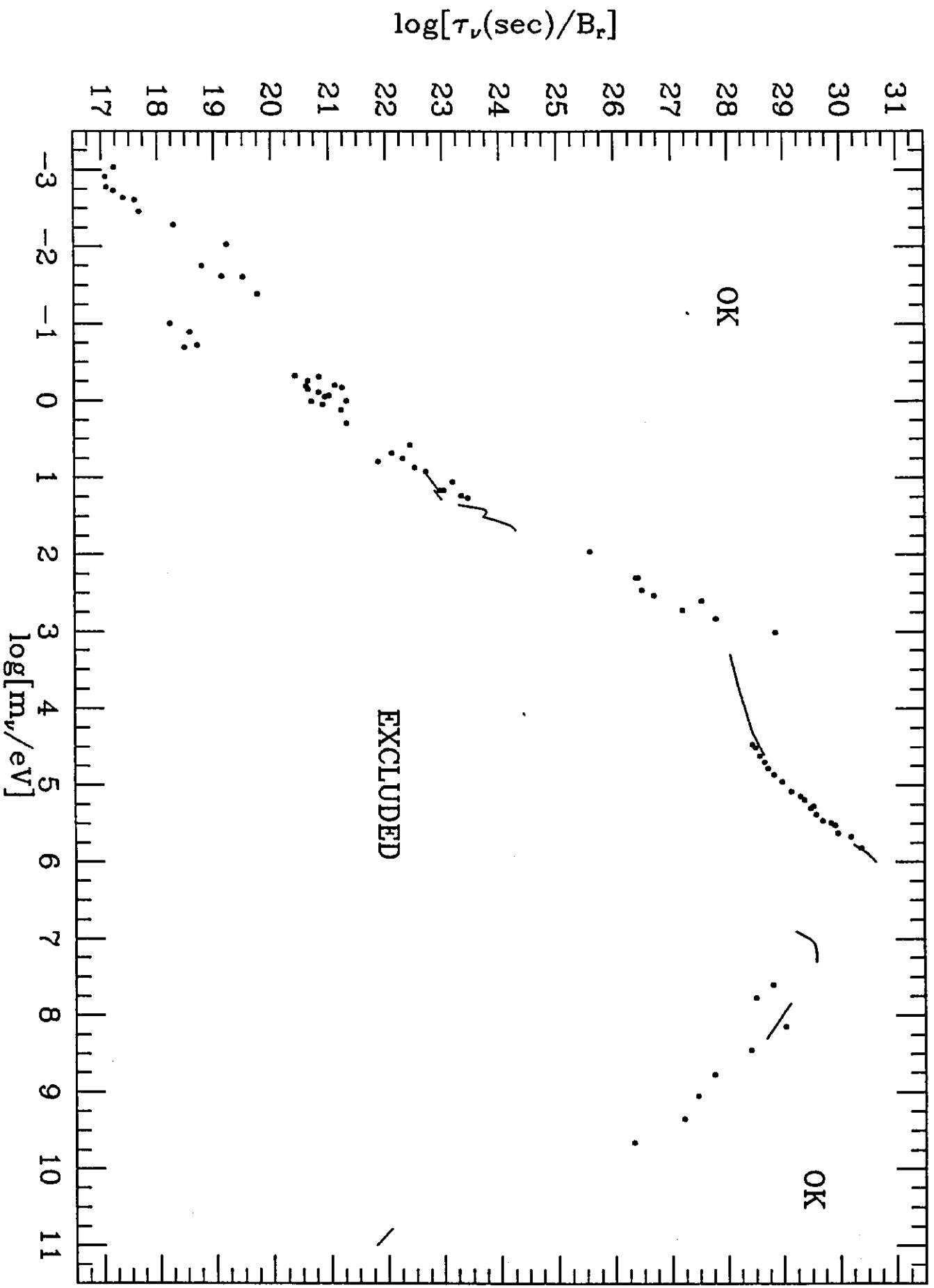
log[τ_ν(sec)/B_r]
17
18
19
20
21
22
23
24
25
26
27
28
29
30
31
−3
−2
−1
0
1
2
3
4
5
6
7
8
9
10
11
log[m_ν/eV]
OK
EXCLUDED
OK

FIGURE 8

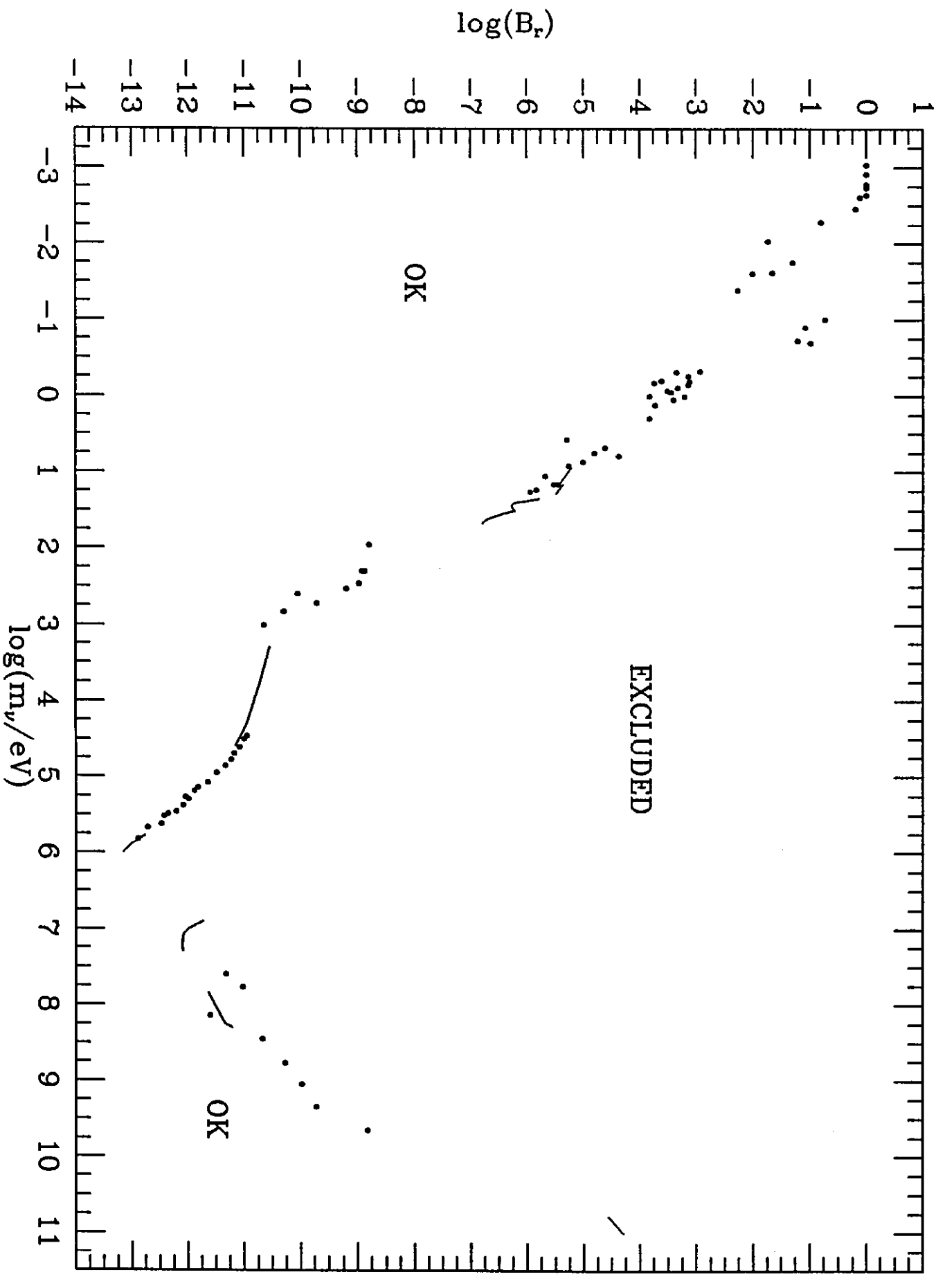
log(B_r)
1
0
−1
−2
−3
−4
−5
−6
−7
−8
−9
−10
−11
−12
−13
−14
−3
−2
−1
0
1
2
3
4
5
6
7
8
9
10
11
log(m_ν/eV)
OK
EXCLUDED
OK

FIGURE 9

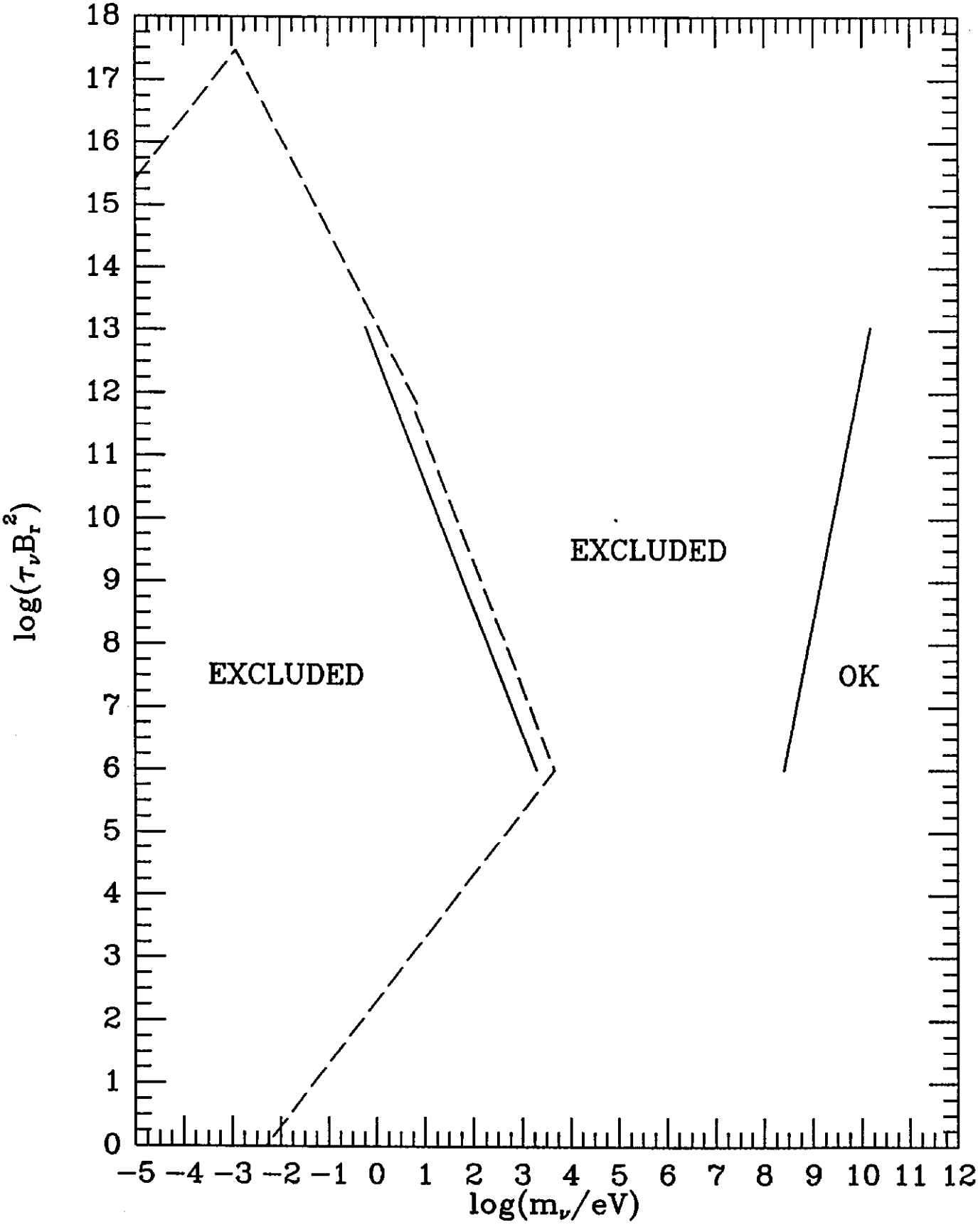
EXCLUDED
EXCLUDED
OK
log(τ_ν B_r^2)
log(m_ν/eV)
18
17
16
15
14
13
12
11
10
9
8
7
6
5
4
3
2
1
0
−5 −4 −3 −2 −1 0 1 2 3 4 5 6 7 8 9 10 11 12

FIGURE 10